Charles University

Faculty of Mathematics and Physics

HABILITATION THESIS

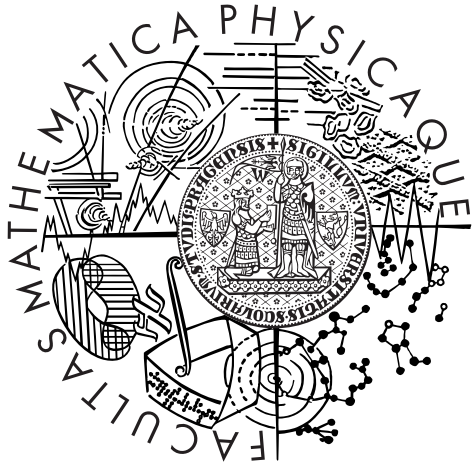

František Němec

Selected wave phenomena in the Earth's inner magnetosphere

Department of Surface and Plasma Science

Physics – Physics of Plasmas

Prague 2016

Contents

Preface

In the presented habilitation thesis, I propose a collection of 30 publications in peer-reviewed impacted international journal of which I am the main author or a coauthor. The presented work has been done primarily at the Department of Surface and Plasma Science of the Faculty of Mathematics and Physics, Charles University in Prague. It concerns the wave phenomena in the space plasma environment, which is my primary scientific focus. My collaboration with Laboratoire de Physique et Chimie de l'Environnement et de l'Espace in Orléans, France (where I defended my Ph.D. thesis in cotutelle) was also crucial for many of the publications. Apart from this, I am actively involved in the analysis of the Martian ionosphere, which is a topic that I started during my postdoctoral fellowship at the Department of Physics and Astronomy of the University of Iowa in Iowa City, Iowa, USA, and which I still continue to pursue. However, in order to keep the theme of the thesis reasonably focused, this – albeit important – part of my research is not discussed here.

All the presented papers use the analysis of recent satellite data to study some of the open topics related to electromagnetic wave phenomena in the space plasma environment surrounding the Earth. We focus in particular on three types of very low frequency wave phenomena, which were the subject of most of my research: equatorial noise emissions, quasiperiodic emissions, and line radiation. All these emissions can be possibly important for the dynamics of the Van Allen radiation belts, and they receive a continuous attention of the community.

Chapter 1

Introduction

Space plasma physics is a part of physics which deals with the plasma environment in the solar system, or, more generally, with the plasma environment anywhere where spacecraft measured in situ data are available. Given the large dimensions of the system, and the absence of any artificial boundaries (which are necessarily present in the case of laboratory experiments), this represents a unique natural laboratory. However, a clear drawback is that there is nearly no way how to modify the system parameters, and we have to rely on what the nature itself provides us with[1].

The principal source of energy which drives the analyzed system is the Sun. Apart from electromagnetic waves, it emanates a steady flow of plasma, so-called solar wind. This plasma consists primarily of protons and electrons, with a small portion (on the order of a few percent) of helium ions. The parameters of the solar wind vary significantly. However, in the long-term average, densities are about 5 cm^{-3} and flow speeds about 400 km/s. The densities are so low that the plasma is practically collisionless. Consequently, once the magnetic field of the solar origin is present in the plasma, it becomes frozen in and it moves along with the plasma flow.

The Earth's intrinsic (roughly dipolar) magnetic field represents an effective obstacle to the incoming solar wind. A pressure balance is set between the dynamic pressure of the solar wind flow and the pressure of the planetary magnetic field. This results in a boundary between the solar wind dominated region and the region controlled by the planetary magnetic field. This characteristic boundary is called "magnetopause", and its location in the subsolar point is usually at a distance of about 10 Earth radii (R_E) from the Earth. The interaction with the solar wind changes significantly the topology of the Earth's magnetic field, which consequently significantly differs from a dipolar configuration, in particular at larger radial distances. Further, as the solar wind flow in the solar system is supersonic, an additional boundary ("bow shock") is formed upstream from the magnetopause (typically at about $13R_E$ in the subsolar point), where the solar wind is abruptly slowed down and becomes more dense.

We focus on the region called "inner magnetosphere", which is the region at radial

[1]Some active experiments focused on modifying the system itself exist(ed), but the modifications are generally rather localized, and such experiments are not a focus of the presented thesis.

distances lower than the magnetopause, where the Earth's magnetic field can be still considered as roughly dipolar. The plasma inside this region is basically 100% ionized, and it consists primarily of electron and hydrogen ions. The nearly dipolar magnetic field configuration allows charged energetic particles to be be efficiently trapped in the inner magnetosphere. Such a magnetic field trapping then results in the formation of so-called Van Allen radiation belts, i.e., regions with a significant population of high energy charged particles. Another important inner-magnetospheric region, this time formed by low energy plasma population, is the "plasmasphere". It is a region where the plasma density (albeit decreasing with increasing radial distance) remains relatively large, $n >\approx 100$ cm^{-3}. Its spatial extent depends significantly on the geomagnetic activity. However, in the equatorial plane, it typically extends up to about $4R_E$ (and it maps along the magnetic field lines to larger geomagnetic latitudes). The outer boundary of the plasmasphere is called "plasmapause". There, the plasma density suddenly drops by an order of magnitude within a few tenths of R_E.

As the analyzed plasma environment is nearly collisionless, thermodynamic equilibrium of individual plasma species can be hardly achieved through collisions. Instead, various plasma instabilities take place. Electromagnetic waves can be generated by unstable particle populations, propagate a considerable distance, and eventually transfer their energy back to the plasma. The understanding of different wave phenomena occurring in the system, in particular their generation mechanisms and propagation patterns, is thus of great importance for understanding the analyzed system. In particular, electromagnetic waves in the Earth's magnetosphere are crucial for the formation of Van Allen radiation belts, being responsible both for particle energization and losses.

There is a large number of different wave phenomena which take place in the Earth's inner magnetosphere. These occur in a broad range of frequencies, from less than 1 Hz up to a few MHz. We focus specifically on waves at frequencies between about 10 Hz and 10 kHz. This frequency range is well covered by recent satellite measurements, and, moreover, the waves in this frequency range are known to be particularly efficient when interacting with radiation belt electrons.

Although we have limited the wave phenomena of interest to the inner magnetosphere and the very low frequency (VLF) range, there is still a substantial number of various wave emissions to be considered. However, among these, we focus exclusively on three particular types of wave phenomena: "equatorial noise" (EN) emissions, "quasiperiodic (QP) emissions", and "line radiation" (LR). These wave phenomena were chosen, because: i) they can be particularly important for electron dynamics in the radiation belts (EN) or their origin is still poorly understood (QP emissions, LR), and ii) detailed wave analysis and multipoint observations available with recent satellite instrumentation can be effectively used for their better understanding. The presented publications cover a long period, from 2004 to 2016. During this time, there was a significant progress in the comprehension of the analyzed phenomena, allowed by a theoretical development, and, most importantly, by new high-resolution and multipoint data sets being available. As an overview of all these phenomena would be too extensive and difficult to follow, it is divided into three chapters, one for each analyzed wave phenomenon.

The satellites, measured data, and related methods of analysis used in our research are shortly described in chapter 2. Individual analyzed wave phenomena will be briefly introduced, and selected main corresponding results obtained will be presented in chapters 3, 4, and 5, respectively. Chapter 6 contains a summary of the presented thesis. All relevant papers of which I am the main author or a coauthor are listed and attached in appendices.

Chapter 2

Spacecraft Data and Analysis

Data from various recent spacecraft were used in the analysis. The performed wave measurements, which are of the main interest, can be of various types. Optimally, waveforms of all six electromagnetic field components are measured. However, due to the limited spacecraft telemetry, these are rarely available. Often, only a waveform of a single component (either electric or magnetic) is measured. Alternatively, in order to further reduce the amount of data needed to be transferred, only a frequency-time spectrogram of power spectral density of field fluctuations (with predefined frequency and time resolutions) is available. Other data relevant for the analysis are plasma number density (and, at lower altitudes, also the plasma composition) and energetic particle measurements.

In the following sections we will briefly introduce individual spacecraft and data used in the analysis. We will also shortly present the most important data analysis methods applied.

2.1 DEMETER

DEMETER was a low-altitude (altitude of about 700 km) spacecraft operating between 2004 and 2010. It had a nearly circular and almost Sun-synchronous orbit (about 10:30 and 22:30 LT), i.e., the measured data were always obtained either close to the local noon or close to the local midnight. The measurements were performed continuously at geomagnetic latitudes lower than about 65°. The wave data (*Berthelier et al.*, 2006a; *Parrot et al.*, 2006) in the VLF range (up to 20 kHz) consisted of an onboard calculated frequency-time spectrograms of one electric and one magnetic field component. These had a frequency resolution of about 20 Hz and a time resolution of about 2 s. Moreover, at specific times, high-resolution ("Burst mode") data were measured. In the VLF range, these consisted of waveforms of one electric and one magnetic field component sampled at 40 kHz. Additionally, in the extra low frequency (ELF, up to 1.25 kHz) range, waveforms of all six electromagnetic field components sampled at 2.5 kHz were available.

Apart from the wave measurements, DEMETER also measured the plasma number density and composition (*Berthelier et al.*, 2006b), and energetic electron flux in a specific

fixed direction (*Sauvaud et al.*, 2006).

2.2 Cluster

The Cluster project (launched in 2000, still active) consists of four spacecraft placed in a close formation on nearly identical elliptical orbits. The orbital parameters have evolved during the course of the mission, but during the first years of operation the apogee was at an altitude of about 119,000 km and the perigee was about 24,000 km. Primarily the data measured during the perigee passes through the equatorial region are thus of interest for performed inner magnetospheric studies. Multicomponent measurements of electromagnetic waves are performed nearly continuously (*Cornilleau-Wehrlin et al.*, 1997, 2003). Three orthogonal magnetic field components and two electric field components in the spin plane of the spacecraft are used for onboard calculation of 5×5 spectral matrices. The analysis is limited to 27 logarithmically spaced frequency channels between 8 Hz and 4 kHz, and the time resolution of the resulting data is about 4 s.

Apart from the low-resolution multicomponent measurements, high-resolution single component data are available during specific time intervals (*Gurnett et al.*, 1997, 2001). These provide us with a waveform band-pass filtered in the frequency range about 70 Hz – 9.5 kHz and sampled with the sampling frequency of 27,443 kHz.

Cluster measurements of the plasma number density (*Décréau et al.*, 1997, 2001) and low-frequency measurements of 3 components of the ambient magnetic field (*Balogh et al.*, 1997, 2001) were also used in some of the performed studies.

2.3 Van Allen Probes

The Van Allen Probes (formerly called Radiation Belt Storm Probes, launched in 2012, still active) are two spacecraft following one the other along nearly identical orbits. The orbits are close to the equatorial plane and highly elliptical, with a perigee of about 600 km and an apogee of as much as about 30000 km. The continuous survey mode data consist of wave intensities and propagation parameters calculated using three magnetic and three electric field components. The time resolution of the data is 6 s, and there are 64 frequency channels spanning the frequency range from 10 Hz up to 12 kHz (*Kletzing et al.*, 2013). Ambient magnetic field measurements with a sampling frequency of 64 kHz are also available. Additionally, the plasma number density may be inferred from the wave measurements (*Kurth et al.*, 2015).

2.4 Data Analysis

Simultaneous measurements of several components of electromagnetic field allow us to perform a detailed wave analysis, i.e., to determine the polarization properties, wave and Poynting vector directions, Poynting flux, etc. (*Santolík et al.*, 2003, 2006). Given density

and magnetic field models, it is possible to perform a raytracing analysis. This essentially allows us to start a wave with a given initial wave vector, and to compute its trajectory in the dispersive plasma medium. Publicly available Tsyganenko (*Tsyganenko*, 1989; *Tsyganenko and Stern*, 1996) magnetic field models provide us with a realistic description of the magnetic field configuration, which is used for tracing the magnetic field lines, and to determine the position of the min-B equator, which is the preferred source region of whistler mode emissions (*Trakhtengerts and Rycroft*, 2008).

Chapter 3

Equatorial Noise

EN emissions (sometimes also called "fast magnetosonic waves") are electromagnetic waves at frequencies between the proton cyclotron frequency and the lower hybrid frequency routinely observed within about 10° from the geomagnetic equator (*Santolík et al.*, 2004; *Němec et al.*, 2005, 2006a) at radial distances between about 2 and 8 R_E (*Ma et al.*, 2013; *Hrbáčková et al.*, 2015; *Xiao et al.*, 2015). They are generated by instabilities of proton distribution functions (*Perraut et al.*, 1982; *McClements and Dendy*, 1993; *McClements et al.*, 1994; *Horne et al.*, 2000; *Chen et al.*, 2011; *Ma et al.*, 2014) and propagate nearly perpendicular to the ambient magnetic field. Although they originally appeared as a noise when observed in low-resolution data (*Russell et al.*, 1970), the analysis of high-resolution data reveals that they consist of a system of harmonic spectral lines related to the proton cyclotron frequency in the source region (*Gurnett*, 1976). These emissions might be important for the dynamics of energetic electrons in radiation belts (*Horne et al.*, 2007; *Bortnik and Thorne*, 2010; *Bortnik et al.*, 2015; *Ma et al.*, 2016; *Shprits*, 2016), and they are thus a subject of intense ongoing research.

3.1 Polarization

An example of an EN event is shown in Figure 3.1. The data were measured by Cluster 4 on 23 April 2002. We use a traditional representation in the form of frequency-time spectrograms, i.e., a color-coded dependence of power spectral density (or other parameter of interest) as a function of frequency (ordinate) and time (abscissa). The used color scale is shown on the right-hand side of the plot. Additionally, selected orbital parameters are plotted on the abscissa along with the time of the measurement.

Five different panels are shown in Figure 3.1. The top panel shows a frequency-time spectrogram of power spectral density of magnetic field fluctuations. Equatorial noise emissions are the intense (red color) emissions at frequencies around 100 Hz whose intensity peaks approximately in the middle of the plotted time interval. The second panel shows the planarity of magnetic field fluctuations, which expresses how well the fluctuations are confined to a single plane, i.e., with an exception of a linearly polarized wave, it indicates

if a plane wave approximation is valid (planarity values close to 1) or if there are several waves propagating in different directions (planarity values close to 0). It can be seen that the values of planarity corresponding to EN emissions are close to 1. The third panel shows the ellipticity of magnetic field fluctuations, i.e., the ratio of minor to major polarization axes. It may range from 0 (linear polarization) to 1 (circular polarization). One can see that the ellipticity of EN emissions is close to 0, i.e., the emissions are nearly linearly polarized. The fourth panel shows the polar angle of wave vector direction with respect to the ambient magnetic field. The values of about 90 degrees correspond to the wave vector nearly perpendicular to the Earth's magnetic field. These propagation parameters were determined using a singular value decomposition (SVD) method (*Santolík et al.*, 2003, 2006).

The last panel of Figure 3.1 shows again a frequency-time spectrogram of power spectral density of magnetic field fluctuations, but this time only for the frequency-time subintervals which fulfill the conditions empirically determined for EN emissions. Specifically, it is required that the planarity of magnetic field fluctuations is larger than 0.8, the ellipticity of magnetic field fluctuations is lower than 0.2, and the wave normal angle is larger than 85°. It can be seen that a simultaneous application of these conditions allows us to identify the part of the spectrogram corresponding to EN emissions extremely well. These polarization properties of EN emissions correspond to the propagation in a so-called extraordinary mode perpendicular to the ambient magnetic field (e.g. *Stix*, 1992). Then, the magnetic field fluctuations are linearly polarized along the ambient magnetic field, and the electric field fluctuations are elliptically polarized in the equatorial plane. The major polarization axis of the electric field polarization ellipse is oriented in the direction of the wave propagation.

Santolík et al. (2004) systematically analyzed polarization properties of electromagnetic emissions observed by the Cluster spacecraft at frequencies lower than 300 Hz, which is an upper estimate of the lower hybrid frequency, i.e., a theoretical maximum frequency of electromagnetic waves propagating perpendicular to the ambient magnetic field in the given mode. They further limited to within ±30° from the geomagnetic equator, which is the region where EN emissions are expected to occur. The used data set consisted of the first two years of Cluster measurements, and it covered radial distances between about 3.9 and 5 R_E. It was found that the ellipticity of intense emissions close to the geomagnetic equator is generally lower than about 0.2, and that the emissions are mainly found within about 10 degrees from the geomagnetic equator. The occurrence rate of EN emissions was estimated to be about 60%.

3.2 Spatial Dependence

The possibility to automatically identify EN emissions using their polarization properties was used in a number of subsequent studies. *Němec et al.* (2005) used first two years of Cluster measurements and an ellipticity threshold to investigate how the intensity of the emissions varies with the geomagnetic latitude. They found that the dependence can be usually approximately described by a Gaussian. The central geomagnetic latitudes of the

intensity distribution are mostly within 2°, and the full-width at half-maximum (FWHM) of the distribution is below 3° in the majority of cases. They further showed that the emissions most often occur at frequencies between about 4 and 5 local proton cyclotron frequencies, with the probability density slowly decreasing toward higher frequencies.

The analysis of the latitudinal dependence of EN intensity was extended by *Němec et al.* (2006a), who used a realistic magnetic field model (*Tsyganenko*, 1989; *Tsyganenko and Stern*, 1996) to demonstrate that incidental deviations of EN intensity peaks from the geomagnetic equator can be explained by problems in determining of the true magnetic equator. Specifically, the distribution of geomagnetic latitudes where the intensity is a maximum gets significantly narrower when a realistic min-B equator is used in place of the dipole geomagnetic latitude. Additionally, the authors demonstrated that the plasma number density can be estimated using the cold plasma theory and measured B/E ratios. The calculated plasma number densities were shown to be reasonably close to the values obtained using the spacecraft potential data.

A global distribution of EN emissions was determined using first 10 years of Cluster data by *Hrbáčková et al.* (2015). Altogether, more than 2000 EN events were identified and analyzed. Importantly, the evolution of the Cluster orbit allowed to investigate a large range of radial distances, from about 1.1 R_E up to about 10 R_E. EN emissions were identified at principally all analyzed radial distances, but their occurrence rate was very low at radial distances lower than 2.5 R_E and at radial distances larger than 8.5 R_E. The occurrence rate was found to be the largest between about 3 and 5.5 R_E and within 7° of the geomagnetic equator, reaching about 40%. The occurrence rate further increased to more than 60% during geomagnetically disturbed periods. As for the magnetic local time (MLT) dependence, a crucial difference between the situation inside and outside the plasmasphere was found. While the occurrence rate inside the plasmasphere is almost independent on MLT, the occurrence rate outside the plasmasphere has a well pronounced peak at about 15 hours MLT.

Němec et al. (2015a) used the same data set as *Hrbáčková et al.* (2015) to analyze intensities of EN events rather than their occurrence rate. They automatically distinguished frequency-time interval with EN emissions using the polarization analysis, and they evaluated the Poynting flux of the emissions in each of the intervals. The intensity of the emissions was then analyzed as a function of possible controlling parameters. It was found that the emissions have higher frequencies and are more intense outside the plasmasphere than inside. Consistent with the occurrence rate results of *Hrbáčková et al.* (2015), the intensity of EN emissions observed in the plasmasphere was found to be nearly independent on MLT, while outisde the plasmasphere the emissions were most intense close to the local noon. This is demonstrated in Figure 3.2, which shows the total intensity of individual EN events as a function of MLT. Figure 3.2a was obtained for the events observed inside the plasmasphere, while Figure 3.2b was obtained for the events observed outside the plasmasphere. We note that locally evaluated plasma densities rather than empirical plasmapause models were used in this study to determine the spacecraft position with respect to the plasmapause. Further, multipoint measurements performed by the Cluster spacecraft allowed to estimate the spatiotemporal variability of EN emissions. It was

shown that although they do not change on the analyzed spatial scales (ΔMLT < 0.2 hours, Δr $< 0.2R_E$), they change considerably on time scales of about an hour.

3.3 Propagation

A possible explanation of the aforementioned MLT dependencies (see section 3.2) stems from the analysis of EN propagation. Raytracing analysis suggests that the emissions can be effectively trapped by the gradients of the refractive index and travel significantly in the azimuth (*Chen and Thorne*, 2012). Consequently, they may be observed at MLTs significantly different from MLTs of their generation, explaining the lack of the MLT dependence inside the plasmasphere. Outside the plasmaphere, no such trapping is possible and the MLT where the emissions are observed likely roughly corresponds to the MLT of their generation.

An experimental analysis of azimuthal directions of EN propagation based on the Cluster spacecraft data was performed by *Němec et al.* (2013a). Due to the specific polarization properties of EN emissions, it was not possible to use the standard method for determining the wave normal direction as a normal to the magnetic field fluctuations. Instead, the elliptical polarization of electric field fluctuations in the equatorial plane, with the major polarization axis oriented in the direction of the wave vector, and the spacecraft rotation (period of about 4 s) were used. High-resolution single component electric field measurements are performed in a plane perpendicular to the spacecraft rotation axis, i.e., approximately in the equatorial plane. Then, as the spacecraft rotates, it periodically sees the minima and maxima of the electric field intensity, depending on the direction of the measured field component with respect to the major polarization axis of electric field fluctuations. This allows to determine the wave vector direction with an ambiguity of $\pm 180°$. Considering also the phases between electric and magnetic field fluctuations, this ambiguity can be resolved.

The results obtained by the analysis of more than 100 EN events for which high-resolution data were available are shown in Figure 3.3. It shows histograms of calculated values of the azimuthal angles of the wave propagation, separated to (a) events measured outside the plasmasphere, and (b) events measured inside the plasmasphere. The distinction between inside/outside plasmasphere was again based on locally evaluated plasma densities. Azimuthal angles of $\pm 90°$ (marked by vertical dashed lines) correspond to the propagation in the eastward/westward direction. It can be seen that while principally isotropic azimuthal directions of EN propagation are observed inside the plasmasphere, wave propagation outside the plasmasphere is directed predominantly to the West or East, i.e., perpendicular to the radial direction. This experimentally determined propagation pattern can be explained by a simple propagation analysis, assuming that the emissions are generated close to the plasmapause. Considering a reasonable density profile around the plasmapause, it can be shown using the cold plasma approximation (*Stix*, 1992) that the refractive index suddenly drops at the plasmapause boundary. A wave impinging on the plasmapause from inside is thus either reflected back to the plasmasphere (for large

enough angles of incidence) or significantly bent toward East/West, consistent with the observations.

Although EN emissions were generally observed and analyzed at larger radial distances, *Santolík et al.* (2016) recently showed, both experimentally and using a raytracing analysis, that such emissions can propagate down to the altitudes of the DEMETER spacecraft (about 700 km). In order to allow for such a propagation down to low altitudes, the original wave vector has to be oriented nearly exactly radially inward. Moreover, the frequency of the waves has to be high enough to be above the $L = 0$ frequency cut-off critically affecting the wave propagation at low altitudes (*Gurnett and Burns*, 1968; *Santolík et al.*, 2006).

3.4 Inner Structure

Although the harmonic frequency structure of EN has been known already for a few decades (*Gurnett*, 1976), they were generally believed to be continuous in time. However, two recent case studies suggested that the emissions may sometimes exhibit a quasiperiodic (QP) time modulation of the wave intensity (*Fu et al.*, 2014; *Boardsen et al.*, 2014). Frequency-time spectrograms of EN emissions may thus resemble frequency-time spectrograms of VLF whistler-mode QP emissions (see chapter 4), which, however, occur at higher frequencies and propagate nearly along the Earth's ambient magnetic field.

Němec et al. (2015b) revealed that a clear QP time modulation of the wave intensity is present in more than 5% of EN events observed by the Cluster spacecraft during the years 2001–2010. The events were found to occur usually in the noon-to-dawn MLT sector, and their occurrence seems to be related to the increased geomagnetic activity, and in particular to enhanced solar wind flow speeds. The modulation period of the events was on the order of minutes. Importantly, compressional ultra low frequency (ULF) magnetic field pulsations with periods about double the modulation periods of EN were identified in about half of the events. It was suggested that these might be possibly responsible for the generation of the events by periodically modulating the wave growth in the source region. High-resolution data were available for some of the events, which enabled to demonstrate that the harmonic frequency structure characteristic for continuous EN events is present also for the EN events with a QP modulation of the wave intensity. An example of such a fine harmonic structure is shown in Figure 3.4. Figure 3.4a shows the frequency-time spectrogram of power spectral density of electric field fluctuations, with several QP wave elements and a fine harmonic frequency structure clearly seen. Figure 3.4b shows the frequency-time plot of the ellipticity of magnetic field fluctuations, in order to demonstrate that the emissions are indeed linearly polarized, as would be the case for normal EN. The identification of the harmonic frequency structure is of a great importance, as it clearly indicates that the generation mechanism of these emissions is not that different from the generation mechanism of normal EN.

Résumé of EN Results

We used a large set of multicomponent wave measurements obtained by the Cluster spacecraft during their equatorial perigee passes to obtain EN spatial dependence and polarization properties. We analyzed EN directions of propagation and we demonstrated the importance of the plasmapause. We showed that EN can propagate down to altitudes of about 700 km, and we systematically investigated properties of EN emissions with a QP time modulation of the wave intensity.

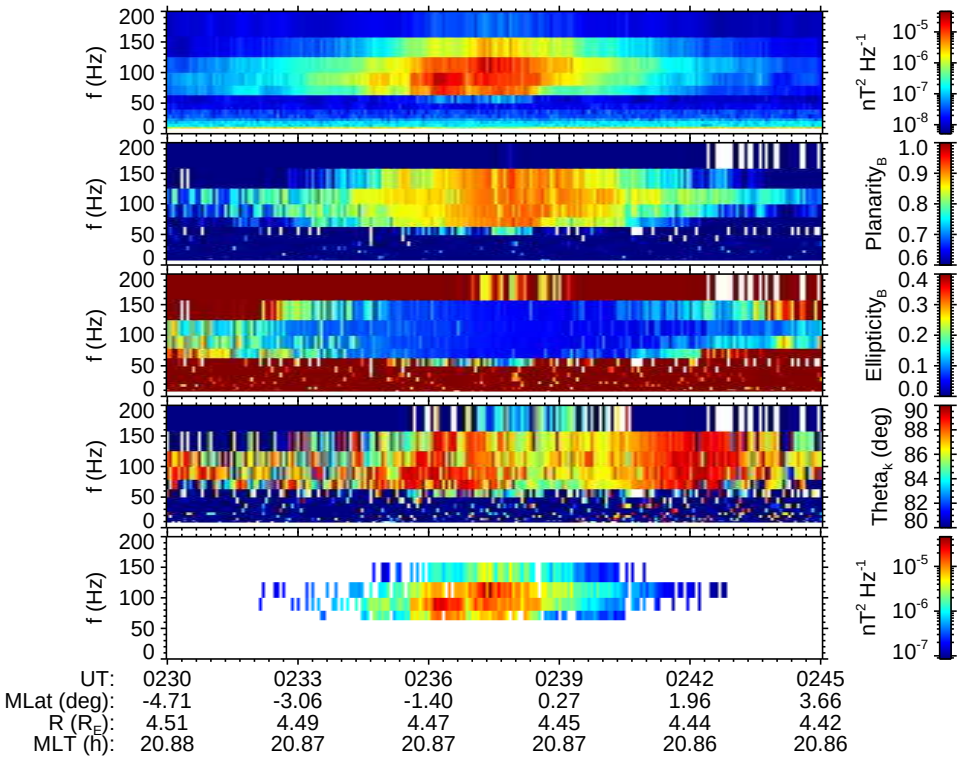

Figure 3.1: Example of an equatorial noise event and related detailed wave analysis. The data were measured on 23 April 2002 by Cluster 4. The individual panels correspond to (from the top) frequency-time spectrogram of power spectral density of magnetic field fluctuations, frequency-time plot of the planarity of magnetic field fluctuations, frequency-time plot of the ellipticity of magnetic field fluctuations, and frequency-time plot of the polar angle of the wave vector direction. The last panel is the same as the first panel (i.e., it shows the frequency-time spectrogram of power spectral density of magnetic field fluctuations), but this time only the frequency-time subintervals that fulfill the conditions set for EN emissions (planarity > 0.8, ellipticity < 0.2, $\theta_k > 85°$) are plotted. Adopted from *Němec et al.* (2013a).

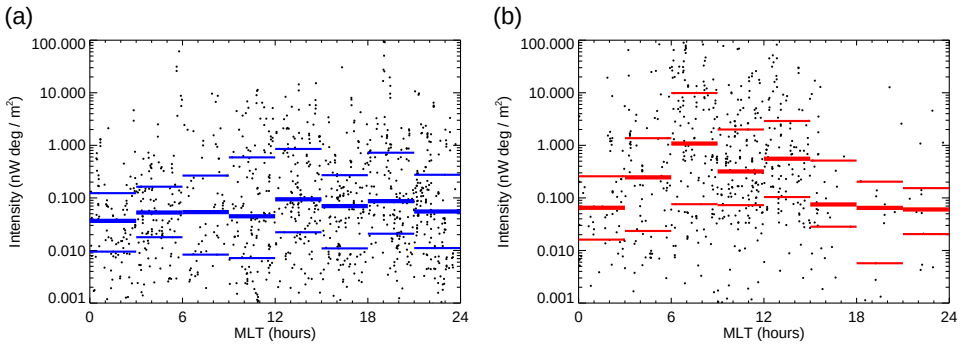

Figure 3.2: Total intensity of individual equatorial noise events as a function of magnetic local time. Thick solid lines correspond to the median dependencies, and thinner solid lines correspond to 0.25 and 0.75 quartiles. (a) Equatorial noise events observed in the plasmasphere. (b) Equatorial noise events observed in the plasma trough. Adopted from *Němec et al.* (2015a).

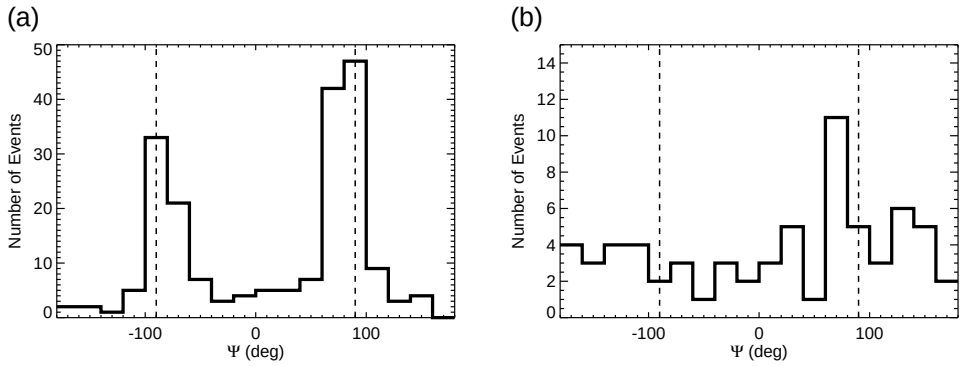

Figure 3.3: Histograms of the calculated values of the azimuthal angles of the wave propagation in the (a) plasma trough and (b) plasmasphere. Azimuthal angles of $\pm 90^\circ$ corresponding to the propagation in the eastward/westward direction are shown by the dashed vertical lines. Adopted from *Němec et al.* (2013a).

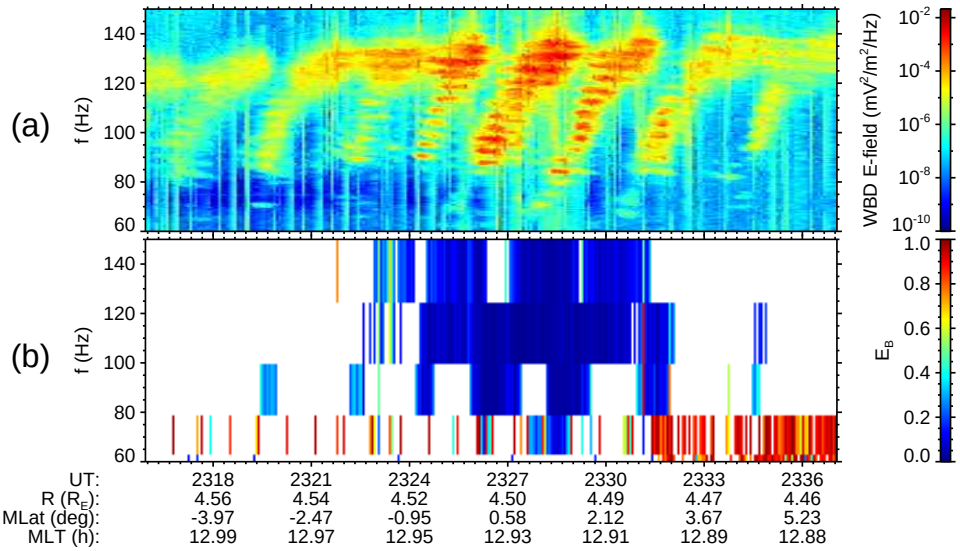

Figure 3.4: Example of an equatorial noise event with a quasiperiodic modulation of the wave intensity observed by Cluster 2 on 23 August 2003 between 23:16 UT and 23:37 UT, when the high-resolution data were available. (a) Frequency-time spectrogram of power spectral density of electric field fluctuations. (b) Frequency-time plot of the ellipticity of magnetic field fluctuations. Adopted from *Němec et al.* (2015b).

Chapter 4

Quasiperiodic Emissions

QP emissions are electromagnetic waves at frequencies between about 0.5 and 4 kHz occurring in the Earth's inner magnetosphere which are characteristic by a periodic time modulation of their intensity. The modulation periods may range from some tens of seconds up to a few minutes (*Sato and Kokubun*, 1980; *Smith et al.*, 1998). They are primarily daytime phenomenon (*Morrison et al.*, 1994; *Engebretson et al.*, 2004). Although they were identified both in the satellite (e.g *Tixier and Cornilleau-Wehrlin*, 1986; *Hayosh et al.*, 2014; *Titova et al.*, 2015) and ground-based data (e.g. *Smith et al.*, 1991; *Manninen et al.*, 2013, 2014), their origin is still unclear. It appears that, at least in some cases, their generation might be related to compressional magnetic field pulsations with a period corresponding to the modulation period of QP emissions, which periodically modulate the growth rate in the source region (*Chen*, 1974; *Sato and Fukunishi*, 1981; *Sazhin*, 1987).

4.1 Occurrence and Propagation Parameters

An example of a QP event measured by Cluster 4 on 13 April 2010 close to the geomagnetic equator is shown in Figure 4.1. Each of the plotted panels corresponds to a 45 minutes long frequency-time spectrogram of power spectral density of electric field fluctuations. QP emissions can be identified during most of the plotted time interval, with their intensity gradually fading at later times.

An inspection of high-resolution data measured by the Cluster spacecraft during the first ten years of the mission at radial distances lower than 10 R_E revealed 21 QP events (*Němec et al.*, 2013c). The frequencies of the events were mostly from about 1 to 4 kHz, but events at frequencies as high as 8 kHz were also identified. Modulation periods of these events were on the order of minutes, with lower periods occurring more frequently. ULF magnetic field pulsations were detected along with the QP emissions in 4 events. Their frequencies roughly corresponded to the modulation periods of the events, suggesting a link between the two phenomena.

Low-resolution multicomponent wave measurements performed by the Cluster spacecraft allowed to determine the wave vector directions of the emissions. It was found that

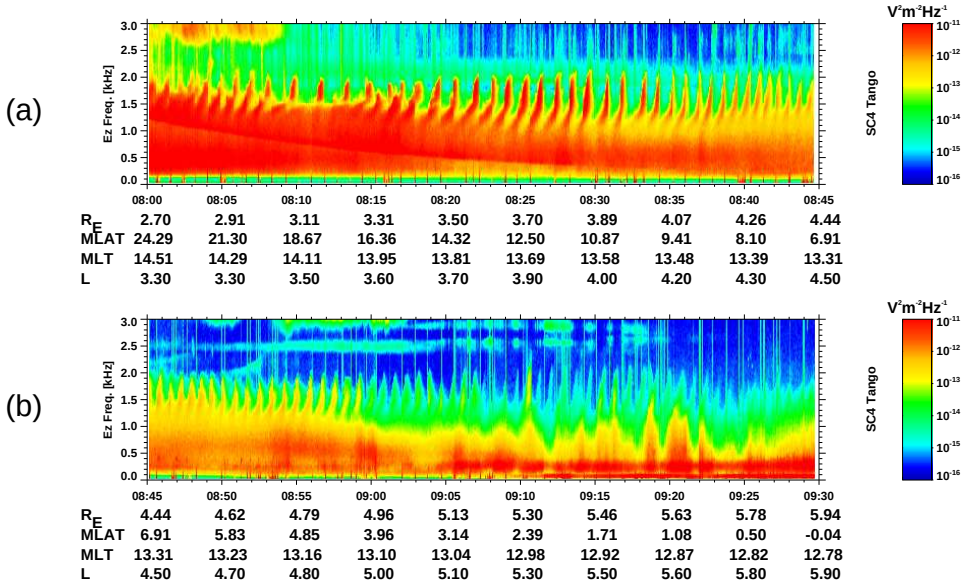

Figure 4.1: High-resolution frequency-time spectrograms of power spectral density of electric field fluctuations measured by Cluster 4 on 13 April 2010 close to the equatorial region at radial distances from about 3 to 6 R_E. Quasiperiodic emissions are observed for most of the plotted time interval, gradually ceasing toward its end. Each of the two panels corresponds to 45 minutes of data. Adopted from *Němec et al.* (2013b).

the wave normal angle exhibits a monotonic variation as a function of the geomagnetic latitude, depicted in Figure 4.2. While the wave vectors are nearly field-aligned close to the geomagnetic equator, they become more oblique at larger geomagnetic latitudes. This clearly shows that the waves propagate unducted.

Considering the low-altitude observations of QP emissions, *Hayosh et al.* (2014) performed a statistical investigation based on all available DEMETER spacecraft data (about 6.5 years of measurements). They showed that the emissions occur in about 5% of daytime DEMETER half-orbits, while they are basically absent during the night. The event occurrence seems to favor quiet geomagnetic conditions following the periods of enhanced geomagnetic activity. The event frequencies were usually between about 0.75 and 2 kHz, but events with frequencies as low as 0.5 kHz and as high as 8 kHz were observed. Interestingly, the event occurrence was found to be significantly (by a factor of more than 2) lower at the longitudes of the South Atlantic magnetic anomaly, which might be related to a massive electron precipitation in the region.

The analysis of propagation properties of QP emissions observed by DEMETER (*Hayosh et al.*, 2016) revealed a rather complicated propagation pattern. The emissions propagate nearly field-aligned at larger geomagnetic latitudes, and they become more oblique at mid-latitudes. It was argued that the observed propagation pattern is consistent with a nonducted propagation from the source located in the equatorial region at larger

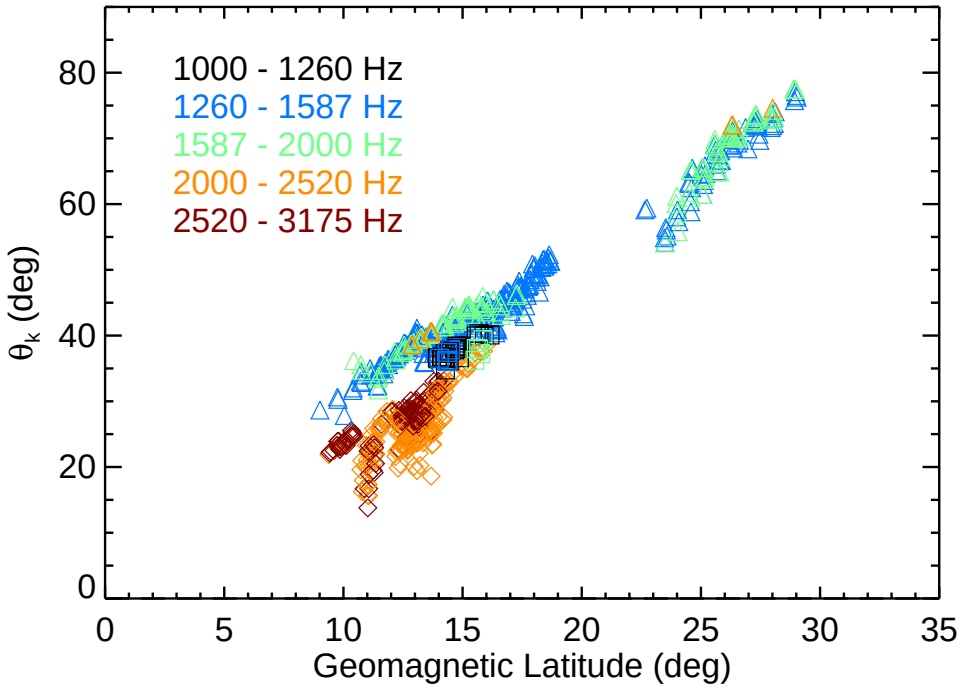

Figure 4.2: Polar angle of the wave vector direction with respect to the ambient magnetic field as a function of the geomagnetic latitude. The wave analysis was done for three different quasiperiodic events (23 April 2002 02:55–03:15, 01 January 2010 13:40–14:15, and 13 April 2010 08:10–08:40). The results obtained for each of them are plotted by a different symbol (diamond, triangle, and square, respectively). The used frequency ranges of are color-coded. Adopted from *Němec et al.* (2013c).

radial distances. The obtained results also provide an indirect evidence of the plasmapause guiding (*Inan and Bell*, 1977) playing an important role in the wave propagation down to low altitudes.

4.2 Multipoint Observations

Multipoint observations of QP emissions (as well as of many other phenomena in space physics) are essential, as they – unlike single point measurements – allow us to distinguish between spatial and temporal variations. Given the number of scientific satellites, their specific orbits, and instrumental limitations, they are, however, quite difficult to achieve. One such conjugate observation of a QP event event performed by Cluster and DEMETER spacecraft was reported by *Němec et al.* (2013b). They showed that the analyzed event lasted for as long as 5 hours, and it spanned over the L-shells from about 1.5 to 5.5. The same QP modulation of the wave intensity was observed at the same time at very different locations in the inner magnetosphere, demonstrating a huge spatial extent of the event.

Further multipoint observations of QP emissions were reported by *Němec et al.* (2014). This study strongly benefited from the 2013 summer Cluster campaign, when a large amount of high-resolution data was measured during the perigee passes through the equatorial region. At the time of the observation, Cluster 1, Cluster 3, and Cluster 4 were very close to each other, while Cluster 2 was located at approximately the same MLT, but about 0.5 R_E closer to the Earth. The same QP modulation of the wave intensity was observed by all the Cluster spacecraft, but individual QP elements were detected by Cluster 2 with a time delay of a couple of seconds. *Němec et al.* (2014) argued that this can be explained by the wave propagation from the generation region located at larger radial distances, close to the plasmapause. The idea was supported by a raytracing analysis, as is demonstrated in Figure 4.3. The plasmapause is assumed to be located at a typical distance of 4 R_E. The wave with a frequency of 1500 Hz is started from a radial distance of 3.7 R_E with the wave vector oriented along the Earth's ambient magnetic field. It propagates to larger geomagnetic latitudes until it encounters the plasmapause boundary. Then, it is guided by the plasmapause until it is reflected at lower altitudes, and it propagates back toward the geomagnetic equator. The wave propagation time for this propagation scheme is in agreement with the observed time delays.

The same QP event was later analyzed by *Němec et al.* (2016a), who used not only the Cluster spacecraft data, but also the data measured by the Van Allen Probes and THEMIS spacecraft. An overview of the measurements preformed by individual spacecraft is shown in Figure 4.4. Figure 4.4a shows a frequency-time spectrogram of power spectral density of electric field fluctuations measured by the Cluster 1 spacecraft. Note that as the Cluster spacecraft are close to each other, the data measured by the remaining Cluster spacecraft are (except of the aforementioned time delay of a couple of seconds) principally the same, and they are thus not plotted. Figures 4.4b,c show frequency-time spectrograms of power spectral density of magnetic field fluctuations measured by Van Allen Probes A and B, respectively. Finally, Figure 4.4d shows a frequency-time spectrogram of power spectral density of magnetic field fluctuations measured by the THEMIS E spacecraft, which is yet another spacecraft which performed wave measurements in the inner magnetosphere at a given time.

The QP event is observed simultaneously by all the spacecraft. However, the spacecraft locations are significantly different. Although they were all rather close to the equatorial plane, the Cluster spacecraft were located on the dawnside at a radial distances of about 3.0–3.5 R_E, and the Van Allen Probes and THEMIS E spacecraft were located on the duskside at radial distances of about 5 R_E and 3.0–4.5 R_E, respectively. This clearly shows that the QP event had a huge spatial extent, both in the radial direction and in the azimuth. It is noteworthy that the analysis of plasma densities measured both by Cluster and Van Allen Probes reveals that all the spacecraft were located in the plasmasphere.

Two phenomena observed in Figure 4.4 are of a particular interest. First, the period of the QP modulation observed by Cluster is about twice lower than the period of the QP modulation observed by the Van Allen Probes and THEMIS E spacecraft. This is likely related to their extremely different MLT, but a possible explanation of this phenomenon is still missing. However, *Němec et al.* (2016a) reported another QP event with a similar

constellation of the spacecraft, and again the modulation period observed by Cluster on the dawnside was about twice lower than the modulation period observed by Van Allen Probes on the duskside. This suggests that the difference between the modulation periods on the dawnside and on the duskside might be a systematic phenomenon.

Another important feature of the QP event from Figure 4.4 is a time delay between individual QP elements as observed by Van Allen Probes and THEMIS E. Specifically, THEMIS E, which is located at later MLTs, observes individual QP elements by about 15 s later. This time delay is too large to be explained by the propagation of the QP emissions. However, it might be explained assuming that the QP modulation is due to an azimuthally propagating compressional ULF wave. The propagation speed of the compressional ULF waves is much lower, in the range of about 300 to 2000 km/s (*Takahashi and McPherron*, 1984; *Tan et al.*, 2011), which would be consistent with the observed time delay. Moreover, as the ULF waves tend to propagate from noon to midnight (*Olson and Rostoker*, 1978; *Chisham and Orr*, 1997), this explanation would be also consistent with the THEMIS E spacecraft observing the QP elements later than Van Allen Probes. Comparable time delays on the order of 10 s likely related to the azimuthal separation were also reported by *Němec et al.* (2016b) using simultaneous satellite and ground-based measurements.

Résumé of QP Emissions Results

We performed a survey of the event occurrence and propagation directions based on the data set obtained by the low-altitude DEMETER spacecraft. We used multipoint measurements (DEMETER, Cluster, Van Allen Probes, and THEMIS spacecraft, and ground-based VLF measurements performed by SGO in Finland) to analyze the spatiotemporal variability of the emissions. We demonstrated that they occur simultaneously over a huge region of the inner magnetosphere. However, the exact timing of individual QP elements was found to be slightly different in different regions. This can be partly explained by the unducted wave propagation from the generation region, partly it is likely due to the propagation of a modulating compressional ULF wave.

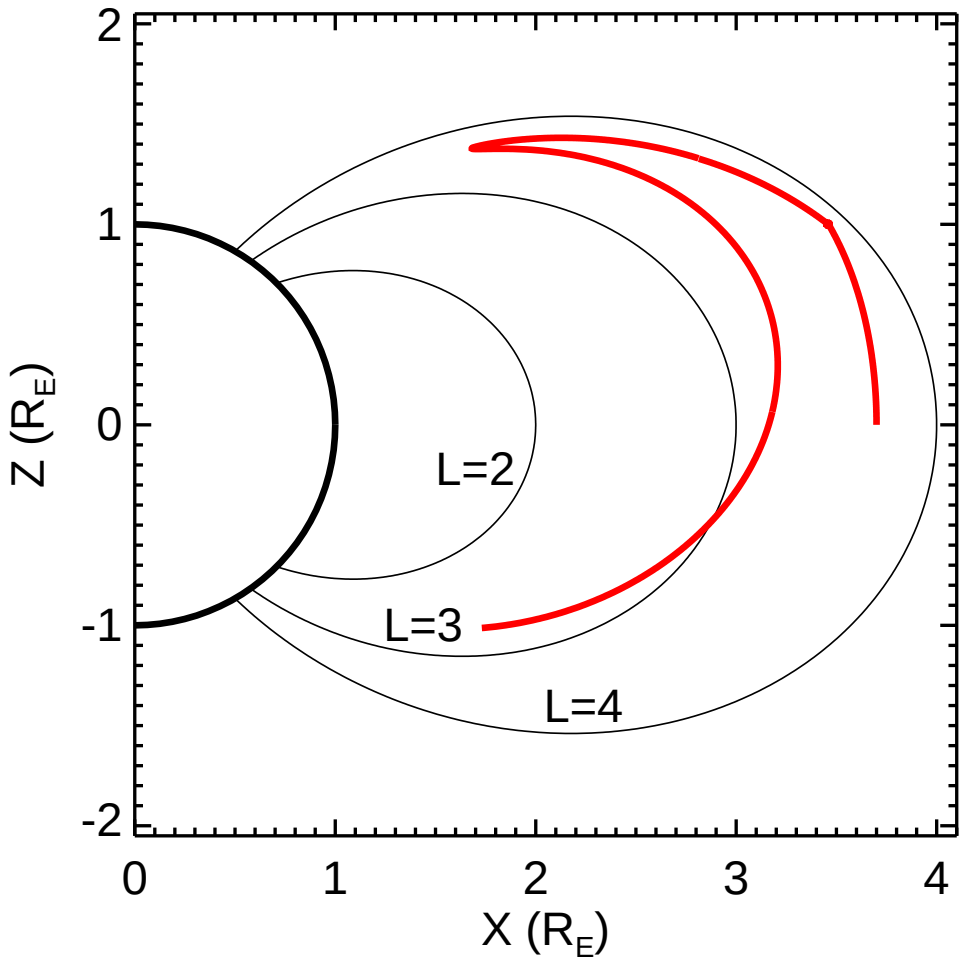

Figure 4.3: Possible scheme of the situation according to the ray tracing analysis. The field-aligned wave with the frequency of 1500 Hz was started at the geomagnetic equator at the radial distance of 3.7 R_E. It encounters the plasmapause density gradient, and it is guided along its inner boundary. Finally, it reflects and propagates to lower latitudes, reaching again the geomagnetic equator, but at lower radial distances. Adopted from *Němec et al.* (2014).

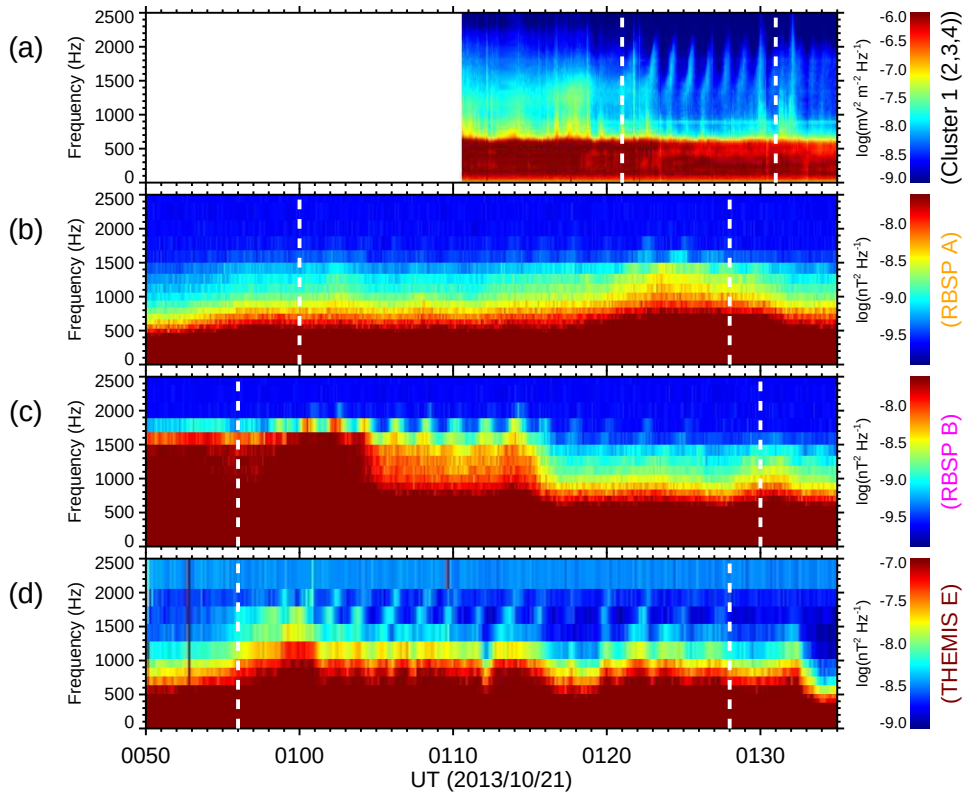

Figure 4.4: Frequency-time spectrograms showing multipoint observations of a quasiperiodic event. The data were obtained on 21 October 2013 between 00:50 UT and 01:35 UT. (a) Frequency-time spectrogram of power spectral density of electric field fluctuations measured by Cluster 1. Note that the white area on the left-hand side corresponds to the missing data due to the fact that high-resolution data were not available at that time. Also note that frequency-time spectrograms measured by other Cluster spacecraft are very similar (see *Němec et al.*, 2014). (b) Frequency-time spectrogram of power spectral density of magnetic field fluctuations measured by Van Allen Probes A. (c) Frequency-time spectrogram of power spectral density of magnetic field fluctuations measured by Van Allen Probes B. (d) Frequency-time spectrogram of power spectral density of magnetic field fluctuations measured by THEMIS E. Adopted from *Němec et al.* (2016a).

Chapter 5

Line Radiation

Frequency spectrum of electromagnetic waves observed in the Earth's inner magnetosphere at frequencies between about 1 and 8 kHz sometimes exhibits a clear harmonic structure. Such events are called line radiation (LR), and they have been observed both by low-altitude satellites (e.g. *Bell et al.*, 1982; *Rodger et al.*, 1995; *Parrot et al.*, 2005) and ground based instruments (e.g. *Rodger et al.*, 1999; *Manninen*, 2005). We note that as compared to EN (which also exhibits a harmonic structure), these events propagate in the whistler mode nearly parallel to the ambient magnetic field. The peak frequencies of some LR events are separated by 50/100 Hz or 60/120 Hz, corresponding to the base frequencies of electric power systems on the ground. Such wave events are due to electromagnetic radiation from power lines on the ground, which penetrates through the ionosphere and can be eventually detected by the spacecraft (*Němec et al.*, 2006b, 2007a, 2008). LR events of this type are usually called Power Line Harmonic Radiation (PLHR). Although they are usually rather week (*Němec et al.*, 2010), there are indications that they could possibly be rather important, as they might serve as triggers for other, more intense emissions (*Nunn et al.*, 1999; *Parrot et al.*, 2014). In fact, there are reports claiming that the magnetosphere behaves differently during weekdays than during weekends, when the power consumption is lower (*Fraser-Smith*, 1979; *Parrot*, 1991). LR events whose frequencies cannot be related to the base frequencies of electric power systems on the ground are called magnetospheric line radiation (MLR). Apart from different frequency spacing, they are usually more intense than PLHR events, their spectral peaks have a larger bandwidth, and the frequencies of these peaks may change over the event duration (*Němec et al.*, 2007b). These events are likely a natural phenomenon (*Rodger et al.*, 2000; *Němec et al.*, 2012a), but some of them might be possibly triggered by PLHR (*Parrot and Němec*, 2009).

5.1 Power Line Harmonic Radiation

5.1.1 Automatic Identification

We have developed a procedure for an automatic identification of PLHR events in the high-resolution DEMETER data (*Němec et al.*, 2006b). Due to the large amount of the data needed to be analyzed, this procedure was implemented and routinely run directly in the DEMETER control center in LPC2E/CNRS, Orléans, France as the level-3 data processing (*Lagoutte et al.*, 2006). Potential PLHR candidates were manually verified, and possible false alarms were excluded. This approach allowed us to obtain the largest data set of spacecraft observations of PLHR events available to date (more than 150 events).

An example of one of the identified PLHR events is shown in Figure 5.1. The top panel shows a frequency-time spectrogram of power spectral density of electric field fluctuations measured by the DEMETER spacecraft on 25 March 2006 after 1913:32 UT. Several thin horizontal lines corresponding to the event, especially well pronounced in the left-hand side of the plot, can be clearly seen. The bottom panel of Figure 5.1 shows the corresponding frequency spectrum. Several intensity peaks located at multiples of the base power system frequency of 50 Hz are marked by the arrows. It is noteworthy that the frequency spacing is 100 Hz, i.e., the intensity peaks are observed only at odd harmonics of the base frequency.

5.1.2 Geographic Distribution

Most of the identified PLHR events had frequencies between about 2 and 3 kHz. They can be further divided into two groups, depending on the frequency spacing between observed harmonic lines. Specifically, while some of the observed events have the frequency spacing of 50/100 Hz, some of the events have the frequency spacing of 60/120 Hz. The geographic locations of the events in respective groups are in excellent agreement with the base power system frequencies used by relevant countries (*Němec et al.*, 2006b, 2007a). This is demonstrated in Figures 5.2 and 5.3. They show geographic locations of the identified PLHR events with the frequency spacing of 50/100 and 60/120 Hz, respectively. The positions of the DEMETER spacecraft at the times of the observations are shown by the large points. Magnetic field lines and footprints of the points of observation are shown by the thin lines and small points. Supposing a ducted wave propagation, the small points indicate possible generation regions. PLHR events with the frequency spacing of 50/100 Hz (Figure 5.2) are observed mostly above Europe. A few of the events are observed to the South from Africa, but their magnetic conjugate point is located again in Europe. PLHR events with the frequency spacing of 60/120 Hz are observed mostly over the United States of America and Japan, a few such events are observed above Brazil. Surprisingly, one such event is observed over New Zealand, whose power systems operate at 50 Hz. However, the magnetic conjugate of the event is in Alaska, where the base power system frequency is 60 Hz.

Němec et al. (2015c) used again the data measured by the DEMETER spacecraft, but they did not focus on the identification and analysis of individual PLHR events. Instead,

they investigated whether the intensity at the harmonics of the base power system frequency (50 Hz or 60 Hz) is increased relative to the nearby frequencies or not. They showed that the intensities of electromagnetic waves detected at frequencies corresponding to the first few harmonics of the base power system frequency are significantly enhanced above industrialized areas. Consistent with the former results, there was an excellent agreement between the frequencies where the wave intensities were increased and base power system frequencies just below the satellite location. The analysis of the measured frequency spectra revealed that the intensity increases are generally limited to odd harmonics of the base power system frequency. A relation of PLHR intensities to geomagnetically induced currents proxy was also demonstrated.

5.1.3 Intensities and Wave Triggering

Němec et al. (2008) fitted individual lines forming the PLHR events by a 2d-Gaussian model. They showed that the mean time duration of the lines forming the events is about 20 s, corresponding to the spatial dimensions of about 150 km. The spectral peaks were generally very thin, with full width at half maximum less than 3 Hz in the majority of cases. *Němec et al.* (2008) further performed a full-wave calculation of the efficiency of coupling of electromagnetic waves from the ground through the ionosphere up to the DEMETER altitudes. The results of such a calculation are shown in Figure 5.4. It shows the efficiency of coupling (i.e., a number between 0 and 1, corresponding to the ratio of the detected to radiated wave intensity) as a function of the altitude. Ionospheric density profiles from the International Reference Ionosphere (IRI) model (*Bilitza*, 1990) and IGRF magnetic field magnitudes were used in the calculation. The efficiency of coupling was evaluated for Finland and Japan regions, i.e., two regions with significantly different geomagnetic latitudes (57.5° and 23°, respectively) where PLHR events are often observed. Moreover, the calculation was performed separately for daytime and nighttime ionospheric conditions. A wave with the frequency of 2.5 kHz, which is a typical frequency of identified PLHR events, was considered.

It is found that the power which penetrates up to the DEMETER altitudes is about five times less attenuated during the night than during the day. Moreover, the efficiency of coupling in the Finland region is larger than in the Japan region, although the difference is far less striking than the day/night asymmetry. The calculated efficiency of coupling of PLHR through the ionosphere can explain the lower intensity of events observed by DEMETER during the day as compared to those observed during the night. Although the estimated radiated peak power during the daytime is larger for the daytime events, consistent with the daytime events occurring more often, they get more attenuated during the propagation through the ionosphere, and the resulting intensity detected by the satellite is thus lower.

A question whether or not PLHR events are intense enough to have a significant effect on the VLF wave activity in the upper ionosphere has been considered in a number of studies (*Parrot and Němec*, 2009; *Němec et al.*, 2010; *Parrot et al.*, 2014). The events analyzed by *Parrot and Němec* (2009) suggested that in some cases PLHR may be responsible

for triggering of MLR events, which can subsequently trigger other associated emissions. Another examples of electromagnetic waves possibly triggered by PLHR were reported by *Parrot et al.* (2014). The triggered emissions had a form of rising tones or hooks with a starting frequency associated to a parent line corresponding to a PLHR event. The events were found to occur preferentially during the daytime, and at frequencies between about 1 and 4 kHz. *Němec et al.* (2010) showed that while the occurrence rate of PLHR events over the industrialized region is quite large (more than 8%), PLHR-triggered emissions appear to be rather rare.

5.2 Magnetospheric Line Radiation

A firm difference between MLR and PLHR events has been established by *Němec et al.* (2007b). Apart from their different frequency spacing, several different properties of the two types of the events were statistically demonstrated. While PLHR events occur both during low and high geomagnetic activity, with none of them being significantly preferred, MLR events occur more frequently under disturbed conditions. Moreover, the frequency bandwidth of individual lines forming the events is significantly larger for MLR than for PLHR. PLHR events are also more intense during the night, while no dependence of MLR peak intensities on MLTs was found. Finally, the lines forming PLHR events are generally constant in frequency, while in the case of MLR events they usually exhibit a frequency drift.

5.2.1 Occurrence and General Properties

An example of a frequency-time spectrogram containing an MLR event is shown in Figure 5.5. It was measured by the DEMETER spacecraft on 10 March 2005, and the plotted data correspond to a full daytime satellite half-orbit. The MLR event is observed at frequencies between about 2.5 and 4 kHz, both in the left-hand and right-hand sides of the plot at large geomagnetic latitudes. Due to the nearly polar satellite orbit, the locations where the event is observed approximately correspond to geomagnetically conjugate regions.

Němec et al. (2009a) presented a survey of about 650 MLR events identified in the first three years of the DEMETER data. The events were found to occur more often during the daytime half-orbits (about 60%) than during the night-time half-orbits, and primarily inside the plasmasphere. Their frequencies usually ranged from about 2 to 6 kHz, . The events were observed mostly at larger geomagnetic latitudes ($L >\approx 2$) and during or after periods of higher geomagnetic activity. Observations of MLR events during several consecutive spacecraft orbits enabled to estimate that in some cases the longitudinal dimensions of the MLR events may be as large as 100°, and the events may last for up to a few hours. Frequency spacing and frequency drifts of individual lines forming the MLR events were investigated by *Němec et al.* (2012a). They showed that neither the frequency spacing nor the frequency drift varies significantly with the L-shell of the observation, and that the frequency drift is generally positive. Importantly, the authors have shown that the individual

lines forming the events cannot be explained as harmonics of the base frequency equal to the frequency spacing. As for the propagation of the emissions, it has been suggested that they might be guided by the plasmapause inner boundary before they deviate to lower L-shells at altitudes of a few thousands of kilometers.

Bezděková et al. (2015) used a superposed epoch analysis to compare the occurrence of 1230 MLR events identified during the whole duration of the DEMETER mission with solar wind parameters and geomagnetic indices. The events were shown to be statistically related to specific solar wind parameters. Additionally, the length of the analyzed time interval was sufficient to allow for investigating the influence of the solar cycle and the season of the year. The events were found to occur more often during the northern winter and spring than during the northern summer. The events also occur less frequently at geomagnetic longitudes of the South Atlantic Anomaly, which is possibly related to a massive electron precipitation in that region. This is demonstrated in Figure 5.6, which shows the longitudinal dependence of the occurrence rate of MLR events by the black curve, and the longitudinal dependence of the precipitating electron flux by the red curve. The analysis of energy spectra of electrons precipitating in this region at the times of MLR events enabled to derive energy-latitude plots of electron flux variations possibly related to the occurrence of MLR events. Finally, high-resolution multicomponent data were available for two of the events, which allowed to perform a detailed wave analysis. It was shown that the events are right-handed nearly circularly polarized, propagating at oblique wave normal angles from larger radial distances and geomagnetic latitudes.

5.2.2 Multipoint Observations

Multipoint observations of the same MLR event are essential to investigate their spatial extent and spatio-temporal variability. However, similarly as for QP emissions (see section 4.2), they are difficult to achieve. The first such observation was reported by *Parrot et al.* (2007), using the data from the DEMETER satellite and ground-based data measured by the instrumentation of the Sodankylä Geophysical Observatory (SGO), Sodankylä, Finland. The analyzed event lasted for as long as two hours, and it was observed over a large area in the Northern hemisphere and in the conjugate region. Another multipoint analysis of an MLR-like event using a combination of the DEMETER and SGO data was presented by *Němec et al.* (2009b). DEMETER observed the event both when flying nearby SGO and in the magnetically conjugate region. The analysis of the timing of high-resolution data allowed to demonstrate that the individual lines forming the event resulted (at least in this particular case) from elements reflected back and forth between the northern and southern hemispheres.

An MLR event observed simultaneously by the Cluster 1, Cluster 2, and DEMETER spacecraft was reported by *Němec et al.* (2012b). At the time of the observation, Cluster 1 and Cluster 2 were located at a radial distance of about 4 R_E not too far from the geomagnetic equator. Although they were separated by as much as 0.7 L-shells, they observed the same frequency-time structure of the emissions. This is demonstrated in Figure 5.7, which shows frequency-time spectrograms of power spectral density of electric field fluctuations

corresponding to the event as observed by Cluster 1 and Cluster 2, respectively. Moreover, as the high-resolution Cluster data periodically cycle between measuring an electric and a magnetic field component, the data at the border of the respective time intervals could be used to estimate the B to E ratios of the emissions. Considering the cold plasma theory and a measured magnetic field magnitude, the observed B to E ratios indicate a quasi-parallel propagation. This suggests that the waves cross the geomagnetic equator over a significant range of radial distances, at least from about 3.9 to 4.6. Finally, simultaneous observations of the same event by the DEMETER spacecraft, which was separated by about 1.8 hours in MLT from the Cluster spacecraft, show a significant azimuthal extent of the event. The obtained results unambiguously demonstrate that during an MLR event the same frequency-time structure of emissions is observed over a significant portion of the inner magnetosphere.

Résumé of LR Results

We demonstrated that there are two distinct types of LR observed in the inner magnetosphere: PLHR and MLR. PLHR events are generated by electromagnetic radiation from electric power systems on the ground, with their geographic distribution and frequency spacings corresponding to those expected based on power systems of individual countries. We also showed that lower PLHR intensities observed during the day are in agreement with larger attenuation in the daytime ionosphere. Although the origin of MLR events remains unexplained, we mapped their global occurrence and properties, and using multi-point observations demonstrated their significant spatial extent.

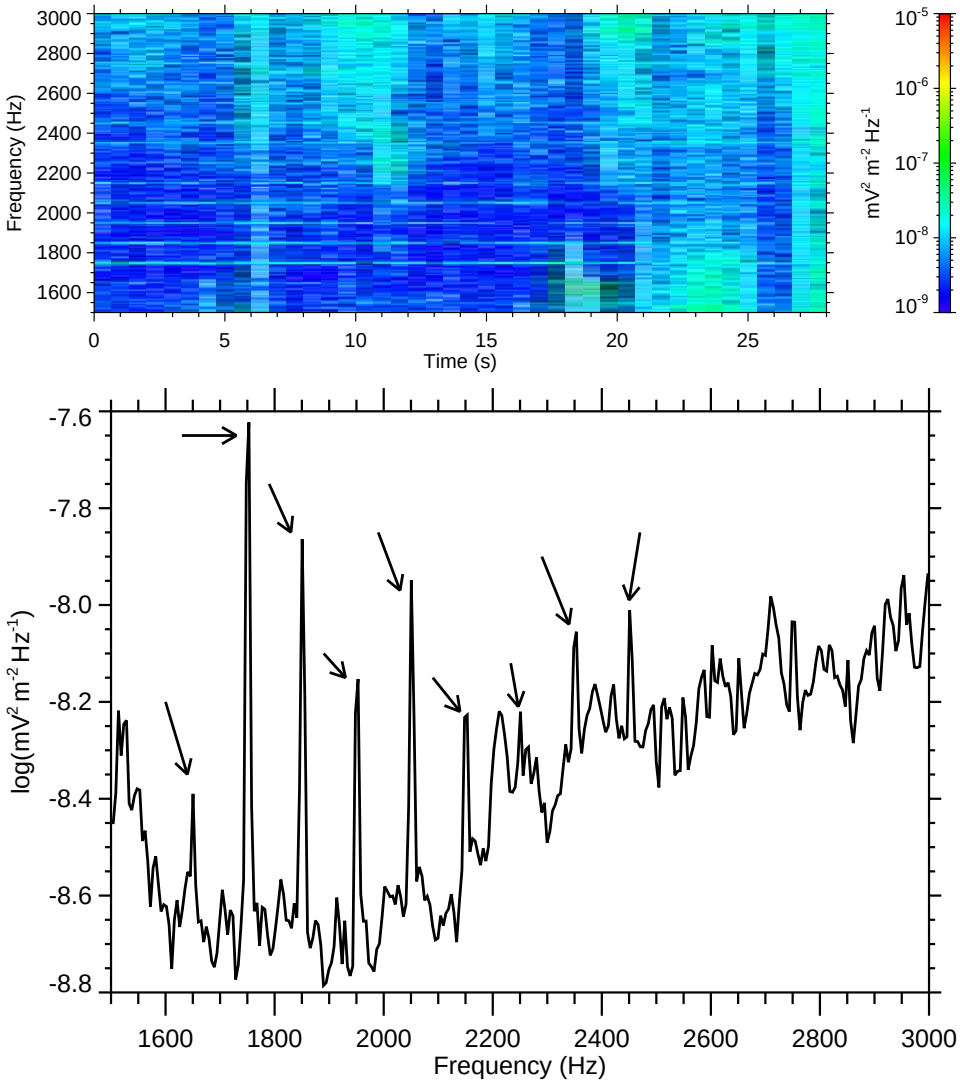

Figure 5.1: Top: An example of frequency-time spectrogram of electric field fluctuations corresponding to one of the analyzed power line harmonic radiation events with 50/100 Hz spacing. The data were recorded on 25 March 2006 from 1913:32 UT when the spacecraft was flying over Finland. Bottom: Power spectrum of the first 18 s of data, with the most important peaks marked by arrows. Adopted from *Němec et al.* (2007b).

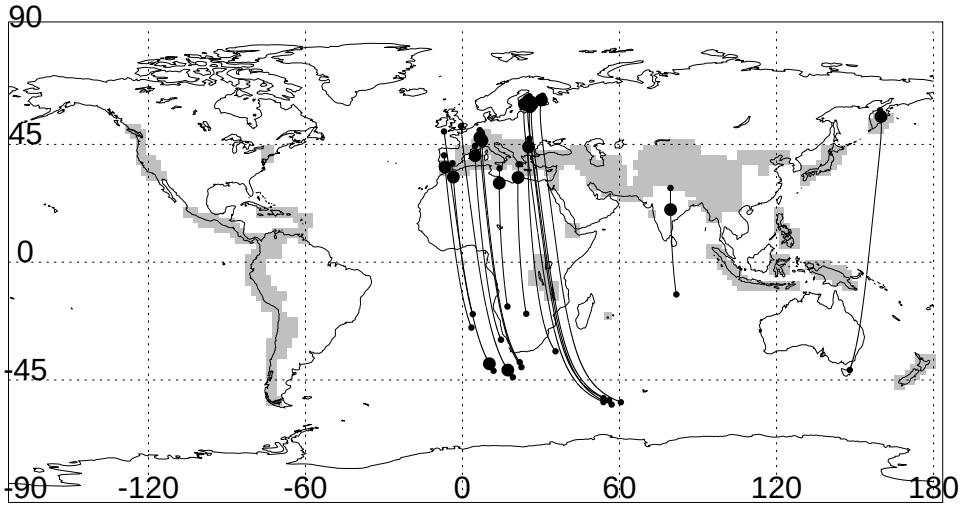

Figure 5.2: Map showing geographic locations of the observed power line harmonic radiation events with the frequency spacing of 50/100 Hz (large points). Magnetic field lines and footprints of the points of observations are plotted by thin lines and small points, respectively. Zones with permanently active Burst mode coverage are shown by gray shading; however, the operational-phase Burst mode regions, which form approximately 20% of the Burst mode data volume, are not shown since their positions vary during the analyzed time interval. Adopted from *Němec et al.* (2007a).

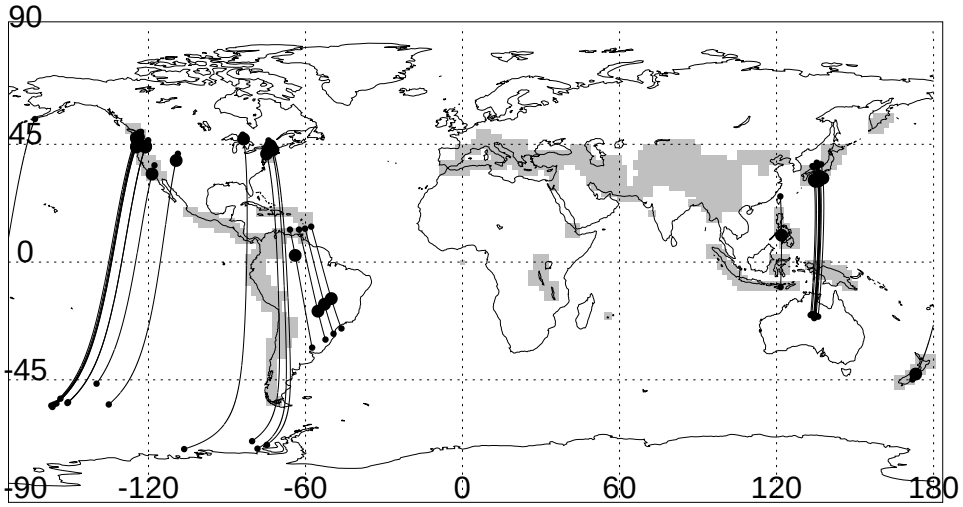

Figure 5.3: Same as Figure 5.2, but for power line harmonic radiation events with the frequency separation of lines 60/120 Hz. Adopted from *Němec et al.* (2007a).

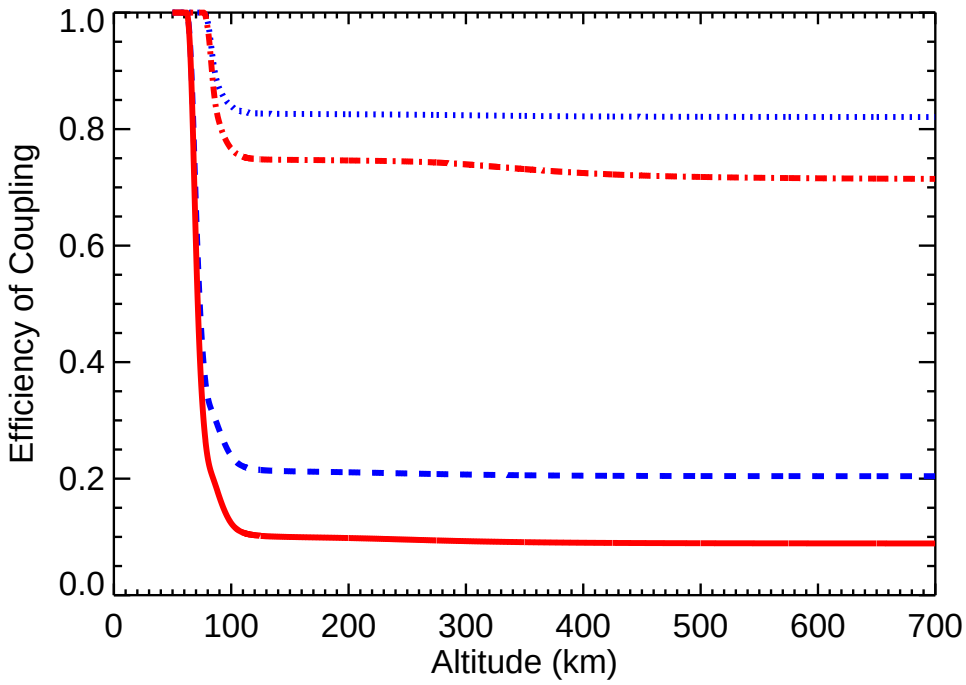

Figure 5.4: Efficiency of coupling for the frequency of wave 2.5 kHz as a function of the altitude for nighttime Finland region (dotted line), nighttime Japan region (dash-dotted line), daytime Finland region (dashed line), and daytime Japan region (solid line). Adopted from *Němec et al.* (2008).

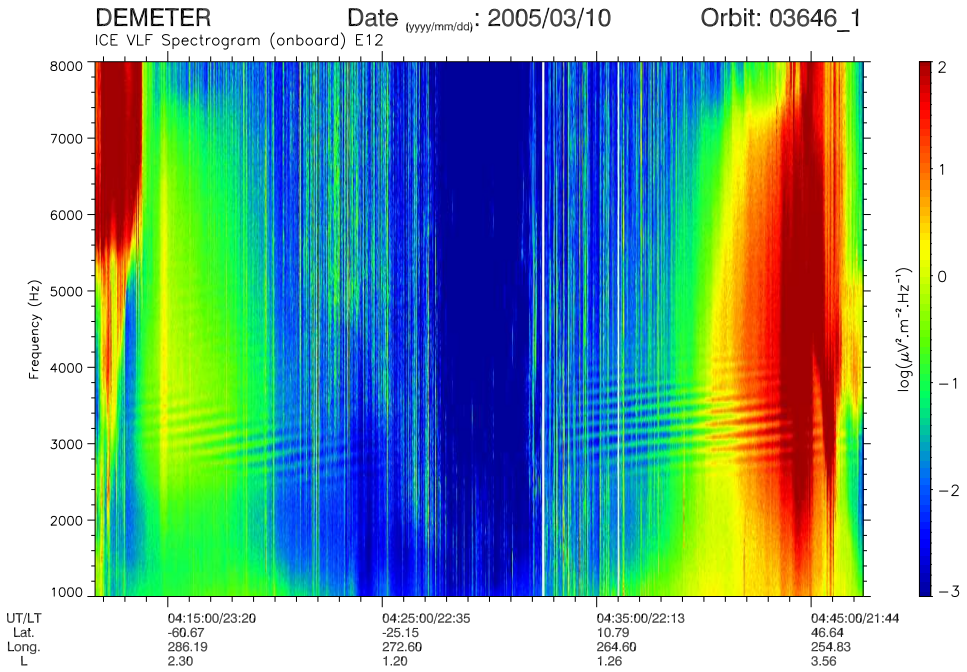

Figure 5.5: An example of a frequency-time spectrogram of a single half-orbit used for the identification of magnetospheric line radiation events. Two magnetospheric line radiation events at frequencies between about 2.5 and 4 kHz can be clearly seen, located in magnetically conjugate regions. Adopted from *Němec et al.* (2009a).

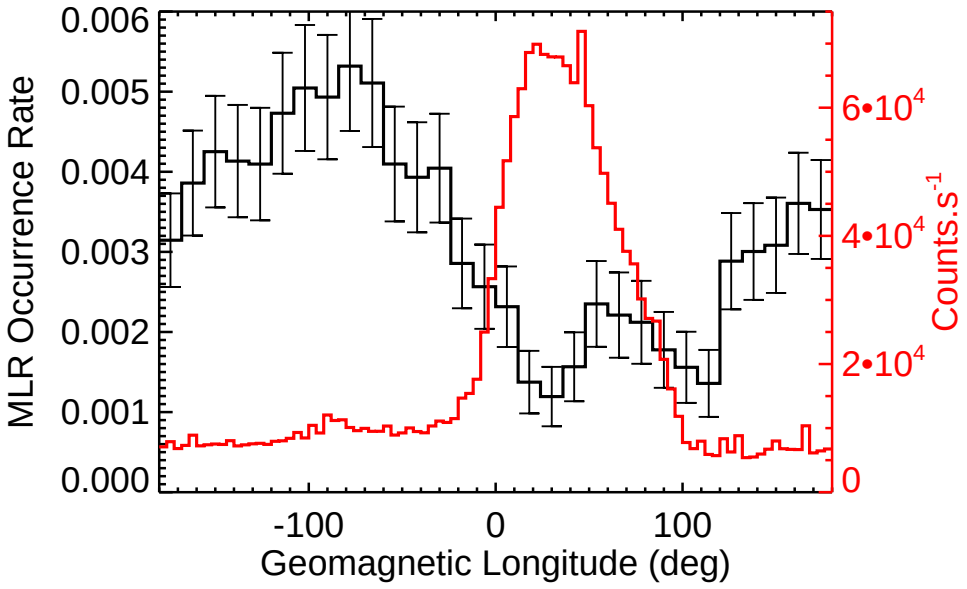

Figure 5.6: Occurrence rate of magnetospheric line radiation events as a function of the geomagnetic longitude is plotted by the black curve using the scale on the left-hand side. The upper estimates of the standard deviations of the occurrence rate in individual longitudinal bins are marked. The red curve (scale on the right-hand side) shows the longitudinal dependence of the mean number of counts per second of energetic electrons with energies between 73 keV and 2342 keV detected by the DEMETER spacecraft. Adopted from *Bezděková et al.* (2015).

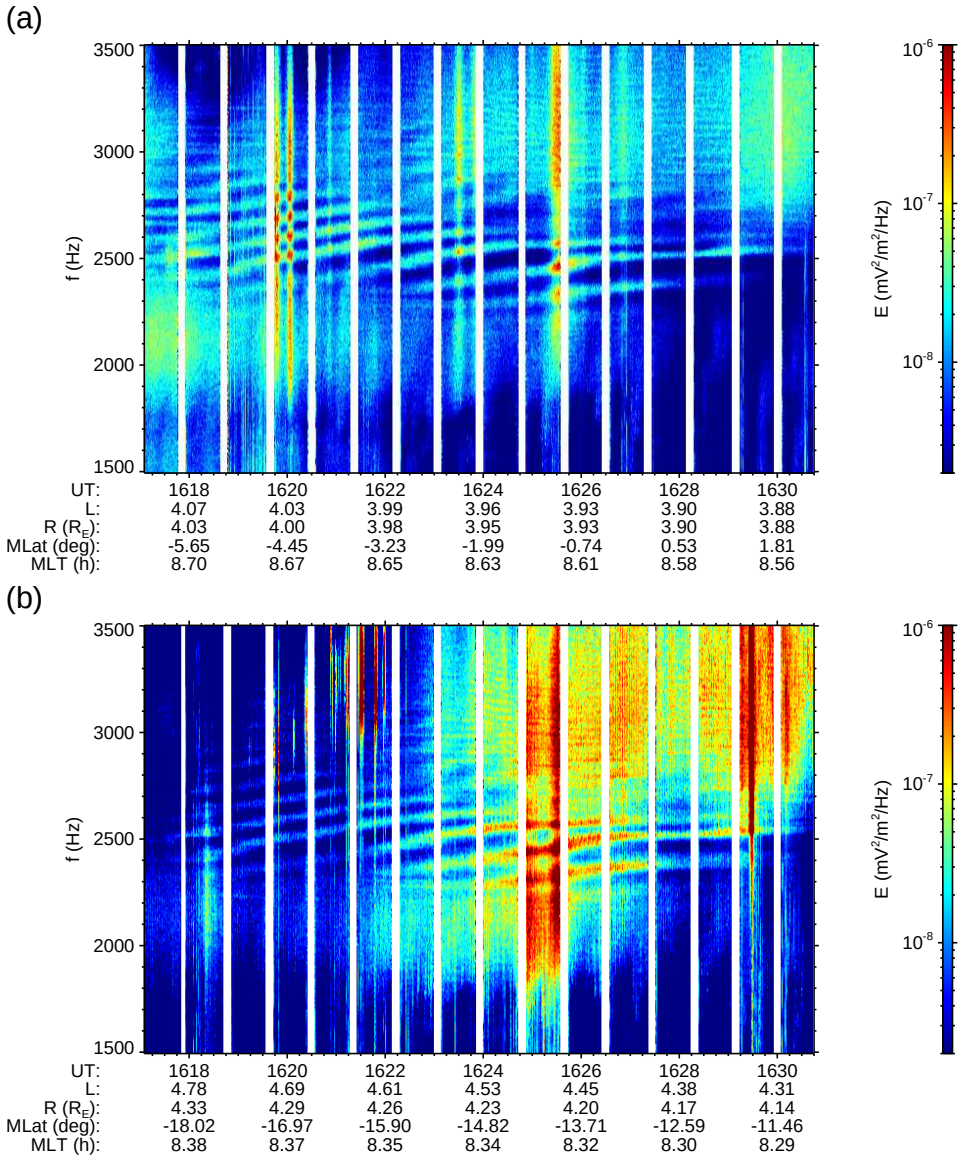

Figure 5.7: Frequency-time spectrograms of power spectral density of electric field fluctuations corresponding to a magnetospheric line radiation event measured by (a) Cluster 1, and (b) Cluster 2 spacecraft. The plotted time interval and the used color scale is the same for both panels. Orbital parameters are provided on the abscissa axis. Adopted from *Němec et al.* (2012b).

Chapter 6

Concluding Remarks

We presented an overview of selected scientific results related to very low frequency waves in the Earth's inner magnetosphere that we have obtained. Three different wave phenomena (equatorial noise, quasiperiodic emissions, and line radiation) were analyzed, and the thesis is structured accordingly. In general, recent satellite data and state-of-the-art methods of analysis have been used to better understand the wave characteristics, their generation mechanisms, and propagation patterns. During the study, we strongly benefited from an intense international collaboration, without which the pursued research would be hardly possible. Apart from the publication in peer-reviewed impacted international journals, the results were continuously presented at international conferences. Several invited talks well document the community interest in the performed research and obtained results.

The main results that we obtained are based on simultaneous measurements by several different spacecraft, which allow us to unambiguously distinguish between spatial and temporal variations. This was used to demonstrate the huge spatial extent of the analyzed phenomena, and, in the case of QP emissions, it allowed us to demonstrate that the exact timing of individual QP elements is slightly different in different regions. We showed that this is partly related to the unducted wave propagation, partly probably to the propagation of a modulating ULF wave. We believe that such multipoint observations are a great promise even for the future, considering that several multispacecraft missions (Cluster, Van Allen Probes, THEMIS) are now simultaneously operating and gathering data in the inner magnetosphere.

Finally, we would like to note that the topic of electromagnetic waves in the Earth's inner magnetosphere and their effects on the radiation belts is hardly closed and there are many remaining unanswered questions. An active research in this field is ongoing not only in our department, but also at many institutes abroad. An intense international cooperation can help to further significantly progress in this field.

References

Balogh, A., M. W. Dunlop, S. W. H. Cowley, D. J. Southwood, J. G. Thomlinson, K. H. Glassmeier, G. Musmann, H. Lühr, S. Buchert, M. H. A. una, D. H. Fairfield, J. A. Slavin, W. Riedler, K. Schwingenschuh, M. Kivelson, and T. C. M. Team (1997), The Cluster magnetic field investigation, *Space Sci. Rev.*, *79*, 65–91, doi:10.1023/A:1004970907748.

Balogh, A., C. M. Carr, M. H. A. na, M. W. Dunlop, T. J. Beek, P. Brown, K. H. Fornacon, E. Georgescu, K.-H. Glassmeier, J. Harris, G. Musmann, T. Oddy, and K. Schwingenschuh (2001), The Cluster magnetic field investigation: an overview of in-flight performance and initial results, *Ann. Geophys.*, *19*, 1207–1217, doi:10.5194/angeo-19-1207-2001.

Bell, T. F., J. P. Luette, and U. S. Inan (1982), ISEE 1 observations of VLF line radiation in the Earth's magnetosphere, *J. Geophys. Res.*, *87*(A5), 3530–3536, doi:10.1029/JA087iA05p03530.

Berthelier, J. J., M. Godefroy, F. Leblanc, M. Malingre, M. Menvielle, D. Lagoutte, J. Y. Brochot, F. Colin, F. Elie, C. Legendre, P. Zamora, D. Benoist, Y. Chapuis, J. Artru, and R. Pfaff (2006a), ICE, the electric field experiment on DEMETER, *Planet. Space Sci.*, *54*, 456–471, doi:10.1016/j.pss.2005.10.016.

Berthelier, J. J., M. Godefroy, F. Leblanc, E. Seran, D. Peschard, P. Gilbert, and J. Artru (2006b), IAP, the thermal analyzer on DEMETER, *Planet. Space Sci.*, *54*, 487–501, doi:10.1016/j.pss.2005.10.018.

Bezděková, B., F. Němec, M. Parrot, O. Santolík, and O. Kruparova (2015), Magnetospheric line radiation: 6.5 years of observations by the DEMETER spacecraft, *J. Geophys. Res. Space Physics*, *120*, 9442–9456, doi:10.1002/2015JA021246.

Bilitza, D. (1990), *International Reference Ionosphere*, NSSDC 90-22, Greenbelt, Maryland.

Boardsen, S. A., G. B. Hospodarsky, C. A. Kletzing, R. F. Pfaff, W. S. Kurth, J. R. Wygant, and E. A. MacDonald (2014), Van Allen Probe observations of periodic rising frequencies of the fast magnetosonic mode, *Geophys. Res. Lett.*, *41*, 8161–8168, doi:10.1002/2014GL062020.

Bortnik, J., and R. M. Thorne (2010), Transit time scattering of energetic electrons due to equatorially confined magnetosonic waves, *J. Geophys. Res.*, *115*(A07213), doi: 10.1029/2010JA015283.

Bortnik, J., R. M. Thorne, B. Ni, and J. Li (2015), Analytical approximation of transit time scattering due to magnetosonic waves, *Geophys. Res. Lett.*, *42*, 1318–1325, doi: 10.1002/2014GL062710.

Chen, L. (1974), Theory of ULF modulation of VLF emissions, *Geophys. Res. Lett.*, *1*(2), 73–75, doi:10.1029/GL001i002p00073.

Chen, L., and R. M. Thorne (2012), Perpendicular propagation of magnetosonic waves, *Geophys. Res. Lett.*, *39*(L14102), doi:10.1029/2012GL052485.

Chen, L., R. M. Thorne, V. K. Jordanova, M. F. Thomsen, and R. B. Horne (2011), Magnetosonic wave instability analysis for proton ring distributions observed by the LANL magnetospheric plasma analyzer, *J. Geophys. Res.*, *116*(A03223), doi: 10.1029/2010JA016068.

Chisham, G., and D. Orr (1997), A statistical study of the local time asymmetry of Pc 5 ULF wave characteristics observed at midlatitudes by SAMNET, *J. Geophys. Res.*, *102*(A11), 24,339–24,350, doi:10.1029/97JA01801.

Cornilleau-Wehrlin, N., P. Chauveau, S. Louis, A. Meyer, J. M. Nappa, S. Perraut, L. Rezeau, P. Robert, A. Roux, C. de Villedary, Y. de Conchy, L. Friel, C. C. Harvey, D. Hubert, C. Lacombe, R. Manning, F. Wouters, F. Lefeuvre, M. Parrot, J. L. Pinçon, B. Poirier, W. Kofman, P. Louarn, and the STAFF Investigator Team (1997), The Cluster spatio-temporal analysis of field fluctuations (STAFF) experiment, *Space Sci. Rev.*, *79*, 107–136, doi:10.1023/A:1004979209565.

Cornilleau-Wehrlin, N., G. Chanteur, S. Perraut, L. Rezeau, P. Robert, A. Roux, C. de Villedary, P. Canu, M. Maksimovic, Y. de Conchy, D. Hubert, C. Lacombe, F. Lefeuvre, M. Parrot, J. L. Pinçon, P. M. E. Décréau, C. C. Harvey, P. Louarn, O. Santolík, H. S. C. Alleyne, M. Roth, T. Chust, O. L. Contel, and S. team (2003), First results obtained by the Cluster STAFF experiment, *Ann. Geophys.*, *21*, 437–456, doi:10.5194/angeo-21-437-2003.

Décréau, P. M. E., P. Fergeau, V. Krasnoselskikh, M. Lévêque, P. Martin, O. Randriamboarison, F. X. Sené, J. G. Trotignon, P. Canu, and P. B. Mögensen (1997), WHISPER, a resonance sounder and wave analyser: Performances and perspectives for the Cluster mission, *Space Sci. Rev.*, *79*(1), 157–193, doi:10.1023/A:1004931326404.

Décréau, P. M. E., P. Fergeau, V. Krasnoselskikh, E. L. Guirriec, M. Lévêque, P. Martin, O. Randriamboarison, J. L. Rauch, F. X. Sené, H. C. Séran, J. G. Trotignon, P. Canu, N. Cornilleau, H. de Féraudy, H. Alleyne, K. Yearby, P. B. Mögensen, G. Gustafsson, M. André, D. C. Gurnett, F. Darrouzet, J. Lemaire, C. C. Harvey, P. Travnicek, and

Whisper experimenters (2001), Early results from the Whisper instrument on Cluster: an overview, *Ann. Geophys.*, *19*, 1241–1258, doi:10.5194/angeo-19-1241-2001.

Engebretson, M. J., J. L. Posch, A. J. Halford, G. A. Shelburne, A. J. Smith, M. Spasojević, U. S. Inan, and R. L. Arnoldy (2004), Latitudinal and seasonal variations of quasiperiodic and periodic VLF emissions in the outer magnetosphere, *J. Geophys. Res.*, *109*(A05216), doi:10.1029/2003JA010335.

Fraser-Smith, A. C. (1979), A weekend increase in geomagnetic activity, *JGR*, *84*, 2089–2096, doi:10.1029/JA084iA05p02089.

Fu, H. S., J. B. Cao, Z. Zhima, Y. V. Khotyaintsev, V. Angelopoulos, O. Santolík, Y. Omura, U. Taubenschuss, L. Chen, and S. Y. Huang (2014), First observation of rising-tone magnetosonic waves, *Geophys. Res. Lett.*, *41*, 7419–7426, doi:10.1002/2014GL061867.

Gurnett, D. A. (1976), Plasma wave interactions with energetic ions near the magnetic equator, *J. Geophys. Res.*, *81*, 2765–2770, doi:10.1029/JA081i016p02765.

Gurnett, D. A., and T. B. Burns (1968), The low-frequency cutoff of ELF emissions, *J. Geophys. Res.*, *73*(23), 7437–7445, doi:10.1029/JA073i023p07437.

Gurnett, D. A., R. L. Huff, and D. L. Kirchner (1997), The wide-band plasma wave investigation, *Space Sci. Rev.*, *79*, 195–208, doi:10.1007/978-94-011-5666-0_8.

Gurnett, D. A., R. L. Huff, J. S. Pickett, A. M. Persoon, R. L. Mutel, I. W. Christopher, C. A. Kletzing, U. S. Inan, W. L. Martin, J.-L. Bougeret, H. S. C. Alleyne, and K. H. Yearby (2001), First results from the Cluster wideband plasma wave investigation, *Ann. Geophys.*, *19*, 1259–1272, doi:10.5194/angeo-19-1259-2001.

Hayosh, M., F. Němec, O. Santolík, and M. Parrot (2014), Statistical investigation of VLF quasiperiodic emissions measured by the DEMETER spacecraft, *J. Geophys. Res. Space Physics*, *119*, 8063–8072, doi:10.1002/2013JA019731.

Hayosh, M., F. Němec, O. Santolík, and M. Parrot (2016), Propagation properties of quasiperiodic VLF emissions observed by the DEMETER spacecraft, *J. Geophys. Res. Space Physics*, *43*, 1007–1014, doi:10.1002/2015GL067373.

Horne, R. B., G. V. Wheeler, and H. S. C. K. Alleyne (2000), Proton and electron heating by radially propagating fast magnetosonic waves, *J. Geophys. Res.*, *105*(A12), 27,597–27,610, doi:10.1029/2000JA000018.

Horne, R. B., R. M. Thorne, S. A. Glauert, N. P. Meredith, D. Pokhotelov, and O. Santolik (2007), Electron acceleration in the Van Allen radiation belts by fast magnetosonic waves, *J. Geophys. Res.*, *34*(L17107), doi:10.1029/2007GL030267.

Hrbáčková, Z., O. Santolík, F. Němec, E. Macúšová, and N. Cornilleau-Wehrlin (2015), Systematic analysis of occurrence of equatorial noise emissions using 10 years of data from the Cluster mission, *J. Geophys. Res. Space Physics*, *120*, 1007–1021, doi: 10.1002/2014JA020268.

Inan, U. S., and T. F. Bell (1977), The plasmapause as a VLF wave guide, *J. Geophys. Res.*, *82*(19), 2819–2827, doi:10.1029/JA082i019p02819.

Kletzing, C. A., W. S. Kurth, M. Acuna, R. J. MacDowall, R. B. Torbert, T. Averkamp, D. Bodet, S. R. Bounds, M. Chutter, J. Connerney, D. Crawford, J. S. Dolan, R. Dvorsky, G. B. Hospodarsky, J. Howard, V. Jordanova, R. A. Johnson, D. I. Kirchner, B. Mokrzycki, G. Needell, J. Odom, D. Mark, R. P. Jr., J. R. Phillips, C. W. Piker, S. L. Remington, D. Rowland, O. Santolik, R. Schnurr, D. Sheppard, C. W. Smith, R. M. Thorne, and J. Tyler (2013), The Electric and Magnetic Field Instrument Suite and Integrated Science (EMFISIS) on RBSP, *Space Sci. Rev.*, *179*, 127–181, doi:10.1007/s11214-013-9993-6.

Kurth, W. S., S. D. Pascuale, J. B. Faden, C. A. Kletzing, G. B. Hospodarsky, S. Thaller, and J. R. Wygant (2015), Electron densities inferred from plasma wave spectra obtained by the Waves instrument on Van Allen Probes, *J. Geophys. Res. Space Physics*, *120*, 904–914, doi:10.1002/2014JA020857.

Lagoutte, D., J. Y. Brochot, D. de Carvalho, F. Elie, F. Harivelo, Y. Hobara, L. Madrias, M. Parrot, J. L. Pinçon, J. J. Berthelier, D. Peschard, E. Seran, M. Gangloff, J. A. Sauvaud, J. P. Lebreton, Š. Štverák, P. Trávníček, J. Grygorczuk, J. Slominski, R. Wronowski, S. Barbier, P. Bernard, A. Gaboriaud, and J. M. Wallut (2006), The DEMETER science mission centre, *Planet. Space Sci.*, *54*, 428–440, doi:10.1016/j.pss.2005.10.014.

Ma, Q., W. Li, R. M. Thorne, and V. Angelopoulos (2013), Global distribution of equatorial magnetosonic waves observed by THEMIS, *Geophys. Res. Lett.*, *40*, 1895–1901, doi: 10.1002/grl.50434.

Ma, Q., W. Li, L. Chen, R. M. Thorne, and V. Angelopoulos (2014), Magnetosonic wave excitation by ion ring distributions in the Earth's inner magnetosphere, *J. Geophys. Res. Space Physics*, *119*, 844–852, doi:10.1002/2013JA019591.

Ma, Q., W. Li, R. M. Thorne, J. Bortnik, C. A. Kletzing, W. S. Kurth, and G. B. Hospodarsky (2016), Electron scattering by magnetosonic waves in the inner magnetosphere, *J. Geophys. Res. Space Physics*, *121*, 274–285, doi:10.1002/2015JA021992.

Manninen, J. (2005), *Some Aspects of ELF-VLF Emissions in Geophysical Research*, 98, Sodankylä Geophysical Observatory Publications, Sodankylä, Finland.

Manninen, J., N. G. Kleimova, O. V. Kozyreva, P. A. Bespalov, and A. E. Kozlovsky (2013), Non-typical ground-based quasi-periodic VLF emissions observed at $L \sim 5.3$

under quiet geomagnetic conditions at night, *J. Atmos. Solar-Terr. Phys.*, *99*, 123–128, doi:10.1016/j.jastp.2012.05.007.

Manninen, J., A. G. Demekhov, E. E. Titova, A. E. Kozlovsky, and D. L. Pasmanik (2014), Quasiperiodic VLF emissions with short-period modulation and their relationship to whistlers: A case study, *J. Geophys. Res. Space Physics*, *119*, 3544–3557, doi: 10.1002/2013JA019743.

McClements, K. G., and R. O. Dendy (1993), Ion cyclotron harmonic wave generation by ring protons in space plasmas, *J. Geophys. Res.*, *98*, 11,689–11,700, doi: 10.1029/93JA00158.

McClements, K. G., R. O. Dendy, and C. N. Lashmore-Davis (1994), A model for the generation of obliquely propagating ULF waves near the magnetic equator, *J. Geophys. Res.*, *99*, 23,685–23,693, doi:10.1029/94JA01979.

Morrison, K., M. J. Engebretson, J. R. Beck, J. E. Johnson, R. L. Arnoldy, J. L. J. Cahill, D. L. Carpenter, and M. Gallani (1994), A study of quasi-periodic ELF-VLF emissions at three Antarctic stations: Evidence for off-equatorial generation?, *Ann. Geophys.*, *12*, 139–146, doi:10.1007/s00585-994-0139-8.

Nunn, D., J. Manninen, T. Turunen, V. Trakhtengerts, and N. Erokhin (1999), On the nonlinear triggering of VLF emissions by power line harmonic radiation, *Ann. Geophys.*, *17*, 79–94, doi:10.1007/s00585-999-0079-4.

Němec, F., O. Santolík, K. Gereová, E. Macúšová, Y. de Conchy, and N. Cornilleau-Wehrlin (2005), Initial results of a survey of equatorial noise emissions observed by the cluster spacecraft, *Planet. Space Sci.*, *53*, 291–298, doi:10.1016/j.pss.2004.09.055.

Němec, F., O. Santolík, K. Gereová, E. Macúšová, H. Laakso, Y. de Conchy, M. Maksimovic, and N. Cornilleau-Wehrlin (2006a), Equatorial noise: Statistical study of its localization and the derived number density, *Adv. Space Res.*, *37*, 610–616, doi: 10.1016/j.asr.2005.03.025.

Němec, F., O. Santolík, M. Parrot, and J. J. Berthelier (2006b), Power line harmonic radiation (PLHR) observed by the DEMETER spacecraft, *J. Geophys. Res.*, *111*(A04308), doi:10.1029/2005JA011480.

Němec, F., O. Santolík, M. Parrot, and J. J. Berthelier (2007a), Power line harmonic radiation: A systematic study using DEMETER spacecraft, *Adv. Space Res.*, *40*, 398–403, doi:10.1016/j.asr.2007.01.074.

Němec, F., O. Santolík, M. Parrot, and J. J. Berthelier (2007b), Comparison of magnetospheric line radiation and power line harmonic radiation: A systematic survey using the DEMETER spacecraft data, *J. Geophys. Res.*, *112*(A04301), doi: 10.1029/2006JA012134.

Němec, F., O. Santolík, M. Parrot, and J. Bortnik (2008), Power line harmonic radiation observed by satellite: Properties and propagation through the ionosphere, *J. Geophys. Res.*, *113*(A08317), doi:10.1029/2008JA013184.

Němec, F., M. Parrot, O. Santolík, C. J. Rodger, M. J. Rycroft, M. Hayosh, D. Shklyar, and A. Demekhov (2009a), Survey of magnetospheric line radiation events observed by the DEMETER spacecraft, *J. Geophys. Res.*, *114*(A05203), doi:10.1029/2008JA014016.

Němec, F., T. Raita, M. Parrot, O. Santolík, and T. Turunen (2009b), Conjugate observations on board a satellite and on the ground of a remarkable MLR-like event, *Geophys. Res. Lett.*, *36*(L22103), doi:10.1029/2009GL040974.

Němec, F., M. Parrot, and O. Santolík (2010), Influence of power line harmonic radiation on the VLF wave activity in the upper ionosphere: Is it capable to trigger new emissions?, *J. Geophys. Res.*, *115*(A11301), doi:10.1029/2010JA015718.

Němec, F., M. Parrot, and O. Santolík (2012a), Detailed properties of magnetospheric line radiation events observed by the DEMETER spacecraft, *J. Geophys. Res.*, *117*(A05210), doi:10.1029/2012JA017517.

Němec, F., O. Santolík, M. Parrot, and J. S. Pickett (2012b), Magnetospheric line radiation event observed simultaneously on board Cluster 1, Cluster 2 and DEMETER spacecraft, *Geophys. Res. Lett.*, *39*(L18103), doi:10.1029/2012GL053132.

Němec, F., O. Santolík, J. S. Pickett, Z. Hrbáčková, and N. Cornilleau-Wehrlin (2013a), Azimuthal directions of equatorial noise propagation determined using 10 years of data from the Cluster spacecraft, *J. Geophys. Res. Space Physics*, *118*, 7160–7169, doi:10.1002/2013JA019373.

Němec, F., O. Santolík, M. Parrot, J. S. Pickett, M. Hayosh, and N. Cornilleau-Wehrlin (2013b), Conjugate observations of quasi-periodic emissions by Cluster and DEMETER spacecraft, *J. Geophys. Res. Space Physics*, *118*, 198–208, doi:10.1029/2012JA018380.

Němec, F., O. Santolík, J. S. Pickett, M. Parrot, and N. Cornilleau-Wehrlin (2013c), Quasiperiodic emissions observed by the Cluster spacecraft and their association with ULF magnetic pulsation, *J. Geophys. Res. Space Physics*, *118*, 4210–4220, doi:10.1002/jgra.50406.

Němec, F., J. S. Pickett, and O. Santolík (2014), Multispacecraft Cluster observations of quasiperiodic emissions close to the geomagnetic equator, *J. Geophys. Res. Space Physics*, *119*, 9101–9112, doi:10.1002/2014JA020321.

Němec, F., O. Santolík, Z. Hrbáčková, and N. Cornilleau-Wehrlin (2015a), Intensities and spatiotemporal variability of equatorial noise emissions observed by the Cluster spacecraft, *J. Geophys. Res. Space Physics*, *120*, 1620–1632, doi:10.1002/2014JA020814.

Němec, F., O. Santolík, Z. Hrbáčková, J. S. Pickett, and N. Cornilleau-Wehrlin (2015b), Equatorial noise emissions with quasiperiodic modulation of wave intensity, *J. Geophys. Res. Space Physics*, *120*, 2649–2661, doi:10.1002/2014JA020816.

Němec, F., M. Parrot, and O. Santolík (2015c), Power line harmonic radiation observed by the DEMETER spacecraft at 50/60 Hz and low harmonics, *J. Geophys. Res. Space Physics*, *120*, 8954–8967, doi:10.1002/2015JA021682.

Němec, F., G. Hospodarsky, J. S. Pickett, O. Santolík, W. S. Kurth, and C. Kletzing (2016a), Conjugate observations of quasiperiodic emissions by the Cluster, Van Allen Probess, and THEMIS spacecraft, *J. Geophys. Res. Space Physics*, *121*, 7647–7663, doi: 10.1002/2016JA022774.

Němec, F., B. Bezděková, J. Manninen, M. Parrot, O. Santolík, M. Hayosh, and T. Turunen (2016b), Conjugate observations of a remarkable quasiperiodic event by the low-altitude DEMETER spacecraft and ground-based instruments, *J. Geophys. Res. Space Physics*, *121*, 8790–8803, doi:10.1002/2016JA022968.

Olson, J. V., and G. Rostoker (1978), Longitudinal phase variations of PC 4–5 micropulsations, *J. Geophys. Res.*, *83*(A6), 2481–2488, doi:10.1029/JA083iA06p02481.

Parrot, M. (1991), Daily variations of ELF data observed by a low-altitude satellite, *Geophys. Res. Lett.*, *18*(6), 1039–1042, doi:10.1029/91GL01352.

Parrot, M., and F. Němec (2009), MLR events and associated triggered emissions observed by DEMETER, *Adv. Space Res.*, *44*, 979–986, doi:10.1016/j.asr.2009.07.001.

Parrot, M., F. Němec, O. Santolík, and J. J. Berthelier (2005), ELF magnetospheric lines observed by DEMETER, *Ann. Geophys.*, *23*, 3301–3311, doi:10.5194/angeo-23-3301-2005.

Parrot, M., D. Benoist, J. J. Berthelier, J. Blecki, Y. Chapuis, F. Colin, F. Elie, P. Fergeau, D. Lagoutte, F. Lefeuvre, C. Legendre, M. Lévêque, J. L. Pincçon, B. Poirier, H. C. Seran, and P. Zamora (2006), The magnetic field experiment IMSC and its data processing onboard DEMETER: Scientific objectives, description and first results, *Planet. Space Sci.*, *54*, 441–455, doi:10.1016/j.pss.2005.10.015.

Parrot, M., J. Manninen, O. Santolík, F. Němec, T. Turunen, T. Raita, and E. Macúšová (2007), Simultaneous observation on board a satellite and on the ground of large-scale magnetospheric line radiation, *Geophys. Res. Lett.*, *34*(L19102), doi: 10.1029/2007GL030630.

Parrot, M., F. Němec, and O. Santolík (2014), Statistical analysis of VLF radio emissions triggered by power line harmonic radiation and observed by the low-altitude satellite DEMETER, *J. Geophys. Res. Space Physics*, *119*, 5744–5754, doi: 10.1002/2014JA020139.

Perraut, S., A. Roux, P. Robert, R. Gendrin, J. A. Sauvaud, J. M. Bosqued, G. Kremser, and A. Korth (1982), A systematic study of ULF waves above f_{H+} from GEOS 1 and 2 measurements and their relationships with proton ring distributions, *J. Geophys. Res.*, *87*, 6219–6236, doi:10.1029/JA087iA08p06219.

Rodger, C. J., N. R. Thomson, and R. L. Dowden (1995), VLF line radiation observed by satellite, *J. Geophys. Res.*, *100*(A4), 5681–5689, doi:10.1029/94JA02865.

Rodger, C. J., M. A. Clilverd, K. H. Yearby, and A. J. Smith (1999), Magnetospheric line radiation observations at Halley, Antarctica, *J. Geophys. Res.*, *104*(A8), 17,441–17,447.

Rodger, C. J., M. A. Clilverd, K. Yearby, and A. J. Smith (2000), Is magnetospheric line radiation man-made?, *J. Geophys. Res.*, *105*, 15,981–15,990, doi:10.1029/1999JA000413.

Russell, C. T., R. E. Holzer, and E. J. Smith (1970), OGO 3 observations of ELF noise in the magnetosphere. the nature of the equatorial noise., *J. Geophys. Res.*, *75*(4), 755–768, doi:10.1029/JA075i004p00755.

Santolík, O., M. Parrot, and F. Lefeuvre (2003), Singular value decomposition methods for wave propagation analysis, *Radio Sci.*, *38*(1), doi:10.1029/2000RS002523.

Santolík, O., F. Němec, K. Gereová, E. Macúšová, Y. de Conchy, and N. Cornilleau-Wehrlin (2004), Systematic analysis of equatorial noise below the lower hybrid frequency, *Ann. Geophys.*, *22*, 2587–2595, doi:10.5194/angeo-22-2587-2004.

Santolík, O., F. Němec, M. Parrot, D. Lagoutte, L. Madrias, and J. J. Berthelier (2006), Analysis methods for multi-component wave measurements on board the DEMETER spacecraft, *Planet. Space Sci.*, *54*, 512–527, doi:10.1016/j.pss.2005.10.020.

Santolík, O., M. Parrot, and F. Němec (2016), Propagation of equatorial noise to low altitudes: Decoupling from the magnetosonic mode, *Geophys. Res. Lett.*, *43*, 6694–6704, doi:10.1002/2016GL069582.

Sato, N., and H. Fukunishi (1981), Interaction between ELF-VLF emissions and magnetic pulsations: Classification of quasi-periodic ELF-VLF emissions based on frequency-time spectra, *J. Geophys. Res.*, *86*(A1), 19–29, doi:10.1029/JA086iA01p00019.

Sato, N., and S. Kokubun (1980), Interaction between ELF-VLF emissions and magnetic pulsations: Quasi-periodic ELF-VLF emissions associated with Pc 3-4 magnetic pulsations and their geomagnetic conjugacy, *J. Geophys. Res.*, *85*(A1), 101–113, doi: 10.1029/JA085iA01p00101.

Sauvaud, J. A., T. Moreau, R. Maggiolo, J.-P. Treilhou, C. Jacquey, A. Cros, J. Coutelier, J. Rouzaud, E. Penou, and M. Gangloff (2006), High-energy electron detection onboard DEMETER: The IDP spectrometer, description and first results on the inner belt, *Planet. Space Sci.*, *54*, 502–511, doi:10.1016/j.pss.2005.10.019.

Sazhin, S. S. (1987), An analytical model of quasiperiodic ELF-VLF emissions, *Planet. Space Sci.*, *35*(10), 1267–1274, doi:10.1016/0032-0633(87)90111-5.

Shprits, Y. Y. (2016), Estimation of bounce resonance scattering by fast magnetosonic waves, *Geophys. Res. Lett.*, *43*, 998–1006, doi:10.1002/2015GL066796.

Smith, A. J., D. L. Carpenter, Y. Corcuff, J. P. S. Rash, and E. A. Bering (1991), The longitudinal dependence of whistler and chorus characteristics observed on the ground near $L = 4$, *J. Geophys. Res.*, *96*(A1), 275–284, doi:10.1029/90JA01077.

Smith, A. J., M. J. Engebretson, E. M. Klatt, U. S. Inan, R. L. Arnoldy, and H. Fukunishi (1998), Periodic and quasiperiodic ELF/VLF emissions observed by an array of Antarctic stations, *J. Geophys. Res.*, *103*(A10), 23,611–23,622, doi:10.1029/98JA01955.

Stix, T. H. (1992), *Waves in Plasmas*, chap. Wave Normal Surfaces, Waves in a Cold Uniform Plasma, pp. 1–46, Springer-Verlag New York, Inc., 175 Fifth Avenue, New York, NY 10010, USA.

Takahashi, K., and R. L. McPherron (1984), Multispacecraft observations of the harmonic structure of Pc 3–4 magnetic pulsations, *J. Geophys. Res.*, *89*(A8), 6758–6774, doi:10.1029/JA089iA08p06758.

Tan, L. C., X. Shao, A. S. Sharma, and S. F. Fung (2011), Relativistic electron acceleration by compressional-mode ULF waves: Evidence from correlated Cluster, Los Alamos National Laboratory spacecraft, and ground-based magnetometer measurements, *J. Geophys. Res.*, *116*(A07226), doi:10.1029/2010JA016226.

Titova, E. E., B. V. Kozelov, A. G. Demekhov, J. Manninen, O. Santolík, C. A. Kletzing, and G. Reeves (2015), Identification of the source of quasiperiodic VLF emissions using ground-based and Van Allen Probes satellite observations, *Geophys. Res. Lett.*, *42*, 6137–6145, doi:10.1002/2015GL064911.

Tixier, M., and N. Cornilleau-Wehrlin (1986), How are the VLF quasi-periodic emissions controlled by harmonics of field line oscillations? The results of a comparison between ground and GEOS satellites measurements, *J. Geophys. Res.*, *91*(A6), 6899–6919, doi:10.1029/JA091iA06p06899.

Trakhtengerts, V. Y., and M. J. Rycroft (2008), *Whistler and Alfvén mode cyclotron masers in space*, p. 354, Cambridge University Press.

Tsyganenko, N. A. (1989), A magnetospheric magnetic field model with a warped tail current sheet, *Planet. Space Sci.*, *37*, 5–20, doi:10.1016/0032-0633(89)90066-4.

Tsyganenko, N. A., and D. P. Stern (1996), Modeling the global magnetic field of the large-scale Birkeland current systems, *J. Geophys. Res.*, *101*(A12), 27,187–27,198, doi:10.1029/96JA02735.

Xiao, F., Q. Zhou, Y. He, C. Yang, S. Liu, D. N. Baker, H. E. Spence, G. D. Reeves, H. O. Funsten, and J. B. Blake (2015), Penetration of magnetosonic waves into the plasmasphere observed by the van allen probes, *Geophys. Res. Lett.*, *42*, 7287–7294, doi:10.1002/2015GL065745.

Appendix A: List of Publications

Equatorial Noise

(EN01) Santolík, O., F. Němec, K. Gereová, E. Macúšová, Y. de Conchy, and N. Cornilleau-Wehrlin (2004), Systematic analysis of equatorial noise below the lower hybrid frequency, *Ann. Geophys.*, *22*, 2587–2595, doi:10.5194/angeo-22-2587-2004.

(EN02) Němec, F., O. Santolík, K. Gereová, E. Macúšová, Y. de Conchy, and N. Cornilleau-Wehrlin (2005), Initial results of a survey of equatorial noise emissions observed by the cluster spacecraft, *Planet. Space Sci.*, *53*, 291–298, doi:10.1016/j.pss.2004.09.055.

(EN03) Němec, F., O. Santolík, K. Gereová, E. Macúšová, H. Laakso, Y. de Conchy, M. Maksimovic, and N. Cornilleau-Wehrlin (2006a), Equatorial noise: Statistical study of its localization and the derived number density, *Adv. Space Res.*, *37*, 610–616, doi:10.1016/j.asr.2005.03.025.

(EN04) Němec, F., O. Santolík, J. S. Pickett, Z. Hrbáčková, and N. Cornilleau-Wehrlin (2013), Azimuthal directions of equatorial noise propagation determined using 10 years of data from the Cluster spacecraft, *J. Geophys. Res. Space Physics*, *118*, 7160–7169, doi:10.1002/2013JA019373.

(EN05) Hrbáčková, Z., O. Santolík, F. Němec, E. Macúšová, and N. Cornilleau-Wehrlin (2015), Systematic analysis of occurrence of equatorial noise emissions using 10 years of data from the Cluster mission, *J. Geophys. Res. Space Physics*, *120*, 1007–1021, doi:10.1002/2014JA020268.

(EN06) Němec, F., O. Santolík, Z. Hrbáčková, and N. Cornilleau-Wehrlin (2015), Intensities and spatiotemporal variability of equatorial noise emissions observed by the Cluster spacecraft, *J. Geophys. Res. Space Physics*, *120*, 1620–1632, doi:10.1002/2014JA020814.

(EN07) Němec, F., O. Santolík, Z. Hrbáčková, J. S. Pickett, and N. Cornilleau-Wehrlin (2015), Equatorial noise emissions with quasiperiodic modulation of wave intensity, *J. Geophys. Res. Space Physics*, *120*, 2649–2661, doi:10.1002/2014JA020816.

(EN08) Santolík, O., M. Parrot, and F. Němec (2016), Propagation of equatorial noise to low altitudes: Decoupling from the magnetosonic mode, *Geophys. Res. Lett.*, *43*, 6694–6704, doi:10.1002/2016GL069582.

Quasiperiodic Emissions

(QP01) Němec, F., O. Santolík, M. Parrot, J. S. Pickett, M. Hayosh, and N. Cornilleau-Wehrlin (2013), Conjugate observations of quasi-periodic emissions by Cluster and DEMETER spacecraft, *J. Geophys. Res. Space Physics*, *118*, 198–208, doi: 10.1029/2012JA018380.

(QP02) Němec, F., O. Santolík, J. S. Pickett, M. Parrot, and N. Cornilleau-Wehrlin (2013), Quasiperiodic emissions observed by the Cluster spacecraft and their association with ULF magnetic pulsation, *J. Geophys. Res. Space Physics*, *118*, 4210–4220, doi:10.1002/jgra.50406.

(QP03) Hayosh, M., F. Němec, O. Santolík, and M. Parrot (2014), Statistical investigation of VLF quasiperiodic emissions measured by the DEMETER spacecraft, *J. Geophys. Res. Space Physics*, *119*, 8063–8072, doi:10.1002/2013JA019731.

(QP04) Němec, F., J. S. Pickett, and O. Santolík (2014), Multispacecraft Cluster observations of quasiperiodic emissions close to the geomagnetic equator, *J. Geophys. Res. Space Physics*, *119*, 9101–9112, doi:10.1002/2014JA020321.

(QP05) Hayosh, M., F. Němec, O. Santolík, and M. Parrot (2016), Propagation properties of quasiperiodic VLF emissions observed by the DEMETER spacecraft, *J. Geophys. Res. Space Physics*, *43*, 1007–1014, doi:10.1002/2015GL067373.

(QP06) Němec, F., G. Hospodarsky, J. S. Pickett, O. Santolík, W. S. Kurth, and C. Kletzing (2016), Conjugate observations of quasiperiodic emissions by the Cluster, Van Allen Probess, and THEMIS spacecraft, *J. Geophys. Res. Space Physics*, *121*, 7647–7663, doi:10.1002/2016JA022774.

(QP07) Němec, F., B. Bezděková, J. Manninen, M. Parrot, O. Santolík, M. Hayosh, and T. Turunen (2016), Conjugate observations of a remarkable quasiperiodic event by the low-altitude DEMETER spacecraft and ground-based instruments, *J. Geophys. Res. Space Physics*, *121*, 8790–8803, doi:10.1002/2016JA022968.

Line Radiation

(LR01) Parrot, M., F. Němec, O. Santolík, and J. J. Berthelier (2005), ELF magnetospheric lines observed by DEMETER, *Ann. Geophys.*, *23*, 3301–3311, doi:10.5194/angeo-23-3301-2005.

(LR02) Němec, F., O. Santolík, M. Parrot, and J. J. Berthelier (2006), Power line harmonic radiation (PLHR) observed by the DEMETER spacecraft, *J. Geophys. Res.*, *111*(A04308), doi:10.1029/2005JA011480.

(LR03) Němec, F., O. Santolík, M. Parrot, and J. J. Berthelier (2007), Comparison of magnetospheric line radiation and power line harmonic radiation: A systematic survey using the DEMETER spacecraft data, *J. Geophys. Res.*, *112*(A04301), doi: 10.1029/2006JA012134.

(LR04) Němec, F., O. Santolík, M. Parrot, and J. J. Berthelier (2007a), Power line harmonic radiation: A systematic study using DEMETER spacecraft, *Adv. Space Res.*, *40*, 398–403, doi:10.1016/j.asr.2007.01.074.

(LR05) Parrot, M., J. Manninen, O. Santolík, F. Němec, T. Turunen, T. Raita, and E. Macúšová (2007), Simultaneous observation on board a satellite and on the ground of large-scale magnetospheric line radiation, *Geophys. Res. Lett.*, *34*(L19102), doi: 10.1029/2007GL030630.

(LR06) Němec, F., O. Santolík, M. Parrot, and J. Bortnik (2008), Power line harmonic radiation observed by satellite: Properties and propagation through the ionosphere, *J. Geophys. Res.*, *113*(A08317), doi:10.1029/2008JA013184.

(LR07) Němec, F., M. Parrot, O. Santolík, C. J. Rodger, M. J. Rycroft, M. Hayosh, D. Shklyar, and A. Demekhov (2009), Survey of magnetospheric line radiation events observed by the DEMETER spacecraft, *J. Geophys. Res.*, *114*(A05203), doi: 10.1029/2008JA014016.

(LR08) Parrot, M., and F. Němec (2009), MLR events and associated triggered emissions observed by DEMETER, *Adv. Space Res.*, *44*, 979–986, doi:10.1016/j.asr.2009.07.001.

(LR09) Němec, F., T. Raita, M. Parrot, O. Santolík, and T. Turunen (2009), Conjugate observations on board a satellite and on the ground of a remarkable MLR-like event, *Geophys. Res. Lett.*, *36*(L22103), doi:10.1029/2009GL040974.

(LR10) Němec, F., M. Parrot, and O. Santolík (2010), Influence of power line harmonic radiation on the VLF wave activity in the upper ionosphere: Is it capable to trigger new emissions?, *J. Geophys. Res.*, *115*(A11301), doi:10.1029/2010JA015718.

(LR11) Němec, F., M. Parrot, and O. Santolík (2012), Detailed properties of magnetospheric line radiation events observed by the DEMETER spacecraft, *J. Geophys. Res.*, *117*(A05210), doi:10.1029/2012JA017517.

(LR12) Němec, F., O. Santolík, M. Parrot, and J. S. Pickett (2012), Magnetospheric line radiation event observed simultaneously on board Cluster 1, Cluster 2 and DEMETER spacecraft, *Geophys. Res. Lett.*, *39*(L18103), doi:10.1029/2012GL053132.

(LR13) Parrot, M., F. Němec, and O. Santolík (2014), Statistical analysis of VLF radio emissions triggered by power line harmonic radiation and observed by the low-altitude satellite DEMETER, *J. Geophys. Res. Space Physics*, *119*, 5744–5754, doi:10.1002/2014JA020139.

(LR14) Němec, F., M. Parrot, and O. Santolík (2015), Power line harmonic radiation observed by the DEMETER spacecraft at 50/60 Hz and low harmonics, *J. Geophys. Res. Space Physics*, *120*, 8954–8967, doi:10.1002/2015JA021682.

(LR15) Bezděková, B., F. Němec, M. Parrot, O. Santolík, and O. Kruparova (2015), Magnetospheric line radiation: 6.5 years of observations by the DEMETER spacecraft, *J. Geophys. Res. Space Physics*, *120*, 9442–9456, doi:10.1002/2015JA021246.